

Carbon nanotube/silicon hybrid heterojunctions for photovoltaic devices

Paola Castrucci*

Department of Physics, University of Roma Tor Vergata, 00133 Roma, Italy

(Received August 2, 2013, Revised January 6, 2014, Accepted January 8, 2014)

Abstract. The significant growth of the Si photovoltaic industry has been so far limited due to the high cost of the Si photovoltaic system. In this regard, the most expensive factors are the intrinsic cost of silicon material and the Si solar cell fabrication processes. Conventional Si solar cells have *p-n* junctions inside for an efficient extraction of light-generated charge carriers. However, the *p-n* junction is normally formed through very expensive processes requiring very high temperature (~1000°C). Therefore, several systems are currently under study to form heterojunctions at low temperatures. Among them, carbon nanotube (CNT)/Si hybrid solar cells are very promising, with power conversion efficiency up to 15%. In these cells, the *p*-type Si layer is replaced by a semitransparent CNT film deposited at room temperature on the *n*-doped Si wafer, thus giving rise to an overall reduction of the total Si thickness and to the fabrication of a device with cheaper methods at low temperatures. In particular, the CNT film coating the Si wafer acts as a conductive electrode for charge carrier collection and establishes a built-in voltage for separating photocarriers. Moreover, due to the CNT film optical semitransparency, most of the incoming light is absorbed in Si; thus the efficiency of the CNT/Si device is in principle comparable to that of a conventional Si one. In this paper an overview of several factors at the basis of this device operation and of the suggested improvements to its architecture is given. In addition, still open physical/technological issues are also addressed.

Keywords: carbon nanotubes; hybrid carbon nanotube/Si heterojunctions; solar cells; photovoltaics

1. Introduction

World energy consumption has been rapidly increasing and power need has now surpassed 15 TW (American Census bureau 2012). At the current growth rate, it is expected that world demand could reach 28 TW by 2050 (Hoffert *et al.* 1998). Nowadays, ~80% of the world-wide energy production comes from fossil fuels. The growing demand for fossil fuels combined with the finite reserves is driving research investments in alternative renewable energy sources. It is targeted that up to 80% of the world's electricity production by 2040 will come from renewable sources (European Energy Council 2006). In this context, solar energy is one of the most promising avenues given its world-wide and constant availability. Current solar electricity production is dominated by the rather mature technology of crystalline silicon solar cells. Despite the efficiency

*Corresponding author, E-mail: paola.castrucci@roma2.infn.it

of the silicon solar cells has steadily improved over the years to approach 16% for multi-Si (Luque and Hegedus 2003) and 25% for mono-Si (Green *et al.* 2012), the significant growth of the Si photovoltaic industry has been limited because of the high cost of the produced Kwh. In the conventional Si solar cell, the *p-n* junction inside acts to efficiently extract the photogenerated charge carriers. The major cost of these devices comes from the Si material and from the expensive and high temperature ($\sim 1000^\circ\text{C}$) requiring fabrication processes, namely processes like ion implantation and annealing or dopant diffusion (U.S. Department of Energy 2010). For these reasons, there is a great interest in looking for solutions that allow the reduction of the Si thickness (and thus the Si total amount) and of the heterojunction fabrication temperature. One of the current scientific and technological challenges to achieve these goals is to combine the well-known properties of Si with low dimensional materials which can be processed at low temperature. Among these novel photovoltaic (PV) devices, carbon nanotube/Si hybrid heterojunctions offer a highly promising avenue for PV research, with potential lower costs and reported power conversion efficiencies (PCE) up to 15% (Shi *et al.* 2012). Carbon nanotubes (CNTs), exhibiting radically different (and sometime unexpected) physical and chemical properties with respect to their bulk counterparts, has prompted an explosive growth in the field of nanostructured materials since the mid-1990s. In particular, CNTs have been studied extensively, due to their peculiar combination of excellent and often unique chemical, optical, electrical and mechanical properties (Mintmire and White 1995, Salvetat *et al.* 1999, Tomblor *et al.* 2000, Liu *et al.* 2000, Wu *et al.* 2004, Fanchini *et al.* 2006, Scarselli *et al.* 2012a). Carbon nanotubes are hollow cylindrical nanostructures composed of one graphene sheet rolled up to form a tube (the so-called single wall carbon nanotube, SWCNTs) or of several SWCNTs concentrically nested into each other (i.e., the multiwall carbon nanotubes, MWCNTs). SWCNTs are characterized by very little diameters, ranging between 0.6 and 2 nm, while their length can reach even several centimeters. Due to their one-dimensional character, they present van Hove singularities in their density of electronic states (Saito *et al.* 1992, Hamada *et al.* 1992, Odom *et al.* 1998, Kim *et al.* 1999, Venema *et al.* 2000). The van Hove singularities are responsible for the unique optical properties observed in SWCNTs. Moreover, they show semiconducting or metallic behaviour depending on their diameter size and on the orientation of the graphene carbon hexagons with respect to the nanotube axis (Dresselhaus *et al.* 1988, Saito *et al.* 1992, Hamada *et al.* 1992). The present paper aims at reviewing the recent developments in the field of carbon nanotube/Si heterojunction photovoltaic devices, paying particular attention to the ones based on crystalline Si. It follows a previous detailed report by Tune *et al.* (2012), that does not cover the interesting results of the last two years due to the rapid evolution in this research area. The present review begins with a brief introduction to carbon nanotubes and their electronic and optical properties, basic concepts that will be useful for a better understanding of the later sections. The subsequent section will briefly report some photovoltaic applications of carbon nanotubes and finally the last section will be dedicated to a review of the carbon nanotube/silicon solar cells.

2. Carbon nanotubes

A single sheet of sp^2 hybridized carbon atoms rolled-up into a hollow cylinder is called a single wall carbon nanotube. A tube consisting of several concentrically arranged cylinders is named multiwall carbon nanotube. SWCNTs have diameters of 0.6-2 nm, while MWCNTs have diameters of 10-30 nm with an interlayer spacing of 0.34 nm. Nanostructures with outer diameter larger than

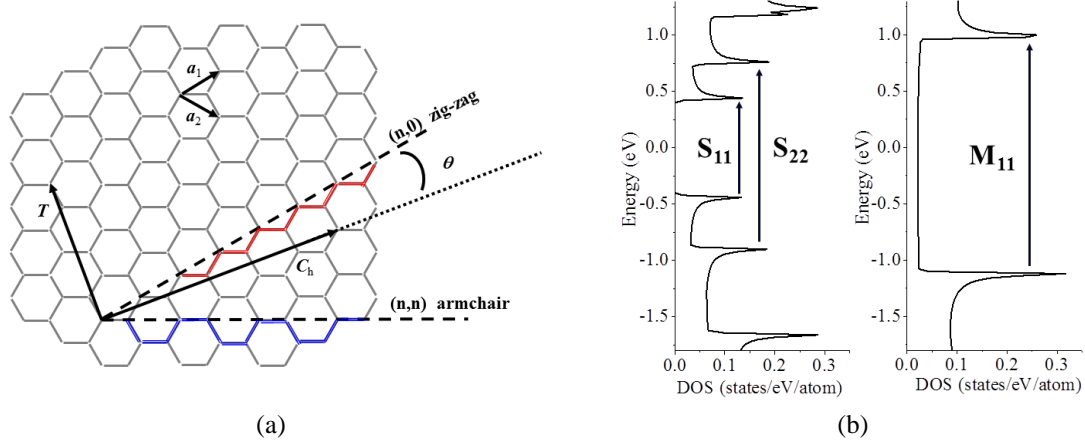


Fig. 1 (a) Graphene honeycomb network with lattice vectors \mathbf{a}_1 and \mathbf{a}_2 . The chiral vector $\mathbf{C}_h = n\mathbf{a}_1 + m\mathbf{a}_2$ represents a possible wrapping of the two-dimensional graphene sheet into a tubular form. The vector, \mathbf{T} , is the translational vector, parallel to the tube axis and perpendicular to \mathbf{C}_h . The chiral angle is defined by the \mathbf{C}_h vector and \mathbf{a}_1 . (b) Schematic of the electronic density of states (DOS) of (left) semiconducting (7,5) and (right) metallic (7,7) SWCNT showing the S_{ii} and M_{ii} transitions between vHs below and above the Fermi level, located at 0 eV energy. Calculated DOS values have been taken from Akai and S. Saito (2005).

30 nm are called carbon nanofibres and possess properties somewhere between carbon fibers and MWCNTs (Jorio *et al.* 2008). The CNT lengths can reach hundreds of micrometers or even centimeters. Single wall carbon nanotubes are univocally described by the circumferential vector of the tube, called the chiral vector (\mathbf{C}_h), which uniquely defines the circumference of the chosen tube and the angle formed by the honeycomb graphene lattice with respect to the tube axis direction. The chiral vector is defined by the equation $\mathbf{C}_h = n\mathbf{a}_1 + m\mathbf{a}_2$, where \mathbf{a}_1 and \mathbf{a}_2 are the unit vectors of the two-dimensional honeycomb graphene lattice wrapped to form the cylinder while the integers (n,m) represents the steps along each unit vector directions, respectively (Fig. 1(a)). The chiral vector \mathbf{C}_h forms the so-called chiral angle, θ , with \mathbf{a}_1 direction. θ can assume values between 0° and 30° . The chiral angle, as well as the pair of indexes (n,m) , determines the geometries of SWCNTs: $\theta = 0^\circ$ or (n,n) nanotubes are called armchair while $\theta = 30^\circ$ or $(n,0)$ nanotubes are named zig-zag, based on the shape of the carbon atom bond arrangement perpendicular to the tube axis (Fig. 1(a)). All the remaining nanotube conformation, with $0^\circ < \theta < 30^\circ$, are referred as chiral nanotubes. Intriguingly, the electronic band structure of single wall carbon nanotubes, and as a consequence their electronic and optical properties, is fully specified by the values of their chiral angle (i.e., the nanotube chirality), or equivalently by the pair of indexes (n,m) . Due to the confinement properties along the SWCNT circumference, the electronic density of states (DOS) exhibits divergences called van Hove singularities (vHs), typical of one-dimensional systems with $(E_0 - E)^{-1/2}$ energy dispersion, and offers the possibility to select, through the (n,m) indices, the metallic or semiconducting behaviors of the nanotubes (Saito 1997, Dresselhaus *et al.* 1996). In particular, SWCNTs behave as metal when $n-m = 3p$ (p is an integer), otherwise they are semiconducting with an energy band gap proportional to the reciprocal of the diameter (Kataura *et al.* 1999). Consequently, most SWCNTs are semiconductors (2/3) and only 1/3 metallic. As an example, Fig. 1(b) reports the calculated DOS of a semiconducting and a

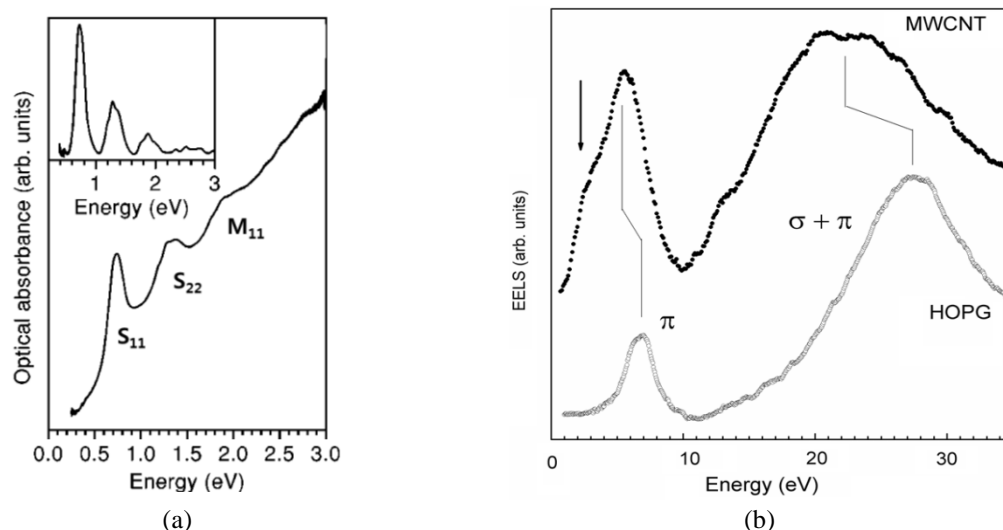


Fig. 2 (a) Optical absorption spectra of the same SWCNT between 0 and 3 eV. The inset shows the absorbance in the range of S_{11} , S_{22} and M_{11} interband transitions after background subtraction. Adapted with permission from Liu *et al.* (2002) Copyright (2002) American Physical Society. (b) Transmission electron energy loss spectra measured by collecting inelastic electrons from a HOPG very thin flake and a MWCNT. Note the shoulder in the MWCNT spectra at energies lower than the plasmon π peak typical of the graphitic systems. Reproduced with permission from Castrucci *et al.* (2011) Copyright (2011) IOP Science

metallic tube (Akai and Saito 2005). In SWCNTs, optical absorption (in case of single particle excitation) occurs between pair of van Hove singularities. Therefore, each nanotube exhibits a typical optical absorption spectrum defined by its (n,m) indexes. In case of semiconducting tubes, S_{ii} are named transitions promoting one electron from the i th singularities below the Fermi energy, E_F , to the i th one above E_F upon photon absorption; M_{ii} those occurring in metallic tubes (with i assuming values from 1 to n as the distance of vHs from E_F increases) (Fig. 1(b)). While S_{ii} energy spans over all the near infrared (NIR), visible (Vis) and near ultraviolet (UV) range, the M_{ii} interband transitions are generally limited to the Vis and the UV regions. All these theoretical findings have been corroborated by a number of experiments performed using techniques as optical absorption spectroscopy (Chen *et al.* 1998, Kataura *et al.* 1999, Liu *et al.* 2002, Murakami *et al.* 2005) and electron energy loss spectroscopy (EELS) (Liu *et al.* 2002) which are able to straightforwardly give information on energies of interband transitions occurring in the SWCNTs. As an example, a typical absorbance spectrum obtained from a SWCNT mat containing both semiconducting and metallic nanotubes of several chiralities is reported in Fig. 2(a). A series of broad absorption peaks are clearly visible in the spectrum, especially after background subtraction (inset of Fig. 2(a)): the most intense of them have been demonstrated to correspond to the three main primary transitions between pairs of van Hove singularities (the S_{11} , the S_{22} , and the M_{11} transitions) while the other peaks between 2 and 3 eV can be assigned to higher energies interband transitions. The wide energy absorption spectrum of SWCNTs made them particularly promising for photovoltaic applications. In the case of MWCNTs, theoretical studies are significantly challenging because of the large number of atoms necessary to model the entire system and of the intertube interactions. In practice, theoretical simulations are very often limited to only double

walled carbon nanotubes (DWCNTs), which represent the most simple model system of MWCNTs (Ho *et al.* 2004, Kwon and Tomanek 1998, Okada and Oshiyama 2003, Saito *et al.* 1993). Therefore, for a long time, MWCNTs have been considered closely related to graphite layers and to exhibit similar electronic properties. The assumed smoothness of MWCNT electronic DOS would not present electronic states able to origin interband transitions upon photon absorption and therefore no MWCNT photocurrent generation.

However, unlike graphite, MWCNTs have been reported to generate a sizeable photocurrent, mostly in the near UV region (Castrucci *et al.* 2006, El Khakani *et al.* 2009). This pinpoints that the electronic DOS of the MWCNTs is considerably different from that of crystalline graphite and suggests the presence of discrete states, due to their reduced dimensionality. In particular, Shyu *et al.* (2000) performed a detailed theoretical calculation simulating EELS spectra and demonstrated that MWCNT electronic properties differ remarkably from those found in graphite. This finding has been confirmed by Castrucci *et al.* (2011) by EELS measurements on individual MWCNTs showing two well defined features at energies between 2.8 and 3.2 eV in addition to the typical π plasmon peak of graphitic systems located, for MWCNTs, around 6 eV (Fig. 2(b)). Moreover, clear hint of electronic occupied states can be observed in the photoemission valence band spectrum of MWCNTs which exhibits a broad feature located around 1 eV (Galimberti *et al.* 2013). In addition, in the same paper, the analysis of i) optical absorption polarisability which, as in the case of SWCNTs (Marukami *et al.* 2005) linearly decreases with photon energy (1.55 - 3 eV) and ii) high-resolution time resolved transmittivity measurements suggest the existence of discrete levels with a well-defined symmetry in the electronic structure of MWCNTs (Galimberti *et al.* 2013). A recent theoretical calculation, performed on carbon nanotubes with 1, 2 and 4 walls showed that the MWCNT density of states can be well reproduced by a superposition of the single wall carbon nanotube DOS constituting the MWCNT structure, each maintaining its one-dimensional features in the electronic and transport properties. As a result, even though the increased number of walls partially smooths out the DOS, discrete broad states may be there still present (Castrucci *et al.* 2011). Moreover, the same calculation predicted that MWCNTs possess a very small density of electronic states at E_F (Castrucci *et al.* 2011) while photoemission valence band and transport experiments indicated that MWCNT networks have a semi-metallic character (Galimberti *et al.* 2013). This means that, contrary to bulk metal cases, excitons with a finite lifetime can be created upon photon absorption. The presence of such discrete states on both sides of the Fermi level together with possibility of exciton existence, may be at the origin of the MWCNT photocurrent generation hereafter discussed.

3. Carbon nanotube photovoltaic properties

In the last twenty years, several research activities have been dedicated to investigate the photovoltaic properties of nanotubes with the aim at exploring their potentialities to be exploited in optoelectronic devices. In fact, optical excitation and recombination across pairs of van Hove singularities, characterized by an energy spacing varying from less than 0.1 to 3 eV, provides the possibility to create nanotube optical detectors or emitters and solar cells that operate across a wide range of optical wavelengths. In this regard, individual nanotube response to the impinging light has been studied as well as the photogeneration properties of nanotube networks. In a rapid sequel, experiments have shown that SWCNT networks are able to generate a photocurrent with peaks in correspondence of the S_{11} and S_{22} transitions (Fujiwara *et al.* 2001) and that photoexcitation across

pairs of van Hove peaks enhances the conductivity of individual semiconductor nanotubes (Freitag *et al.* 2003, Balasubramanian *et al.* 2004). Later, Mohite *et al.* (2005) reported the observation of the M_{11} transition in the photocurrent energy spectrum, evidencing that also metallic nanotubes contribute to photocurrent thus allowing the extension of the spectral response of these nanostructures toward the visible region. Further confirmation of SWCNT ability to origin a photocurrent has been given by Barazzouk *et al.* (2004) who used a SWCNT film as electrode in an electrochemical cell and also showed nanotube maximum contribution to photocurrent in the photon wavelength range between 400 and 500 nm. In addition, it has been recently suggested that the standard limit of photovoltaic efficiency, first established by Shockley and Queisser (1961), setting the conversion of a single photon into electron-hole ($e-h$) pair, can be overcome for carbon nanotubes. In fact, efficient multiple exciton generation (MEG) in carbon nanotubes upon single photon absorption has been shown to occur in (6,5) SWCNTs under 335 nm and 400 nm excitation through pure optical pump and probe experiments (Wang *et al.* 2010) and in individual SWCNT based photodiodes (Gabor *et al.* 2009). On the other hand, solar cells need to be efficient not only in $e-h$ pair generation but also in the subsequent carrier separation and transport. Intrinsically carbon nanotubes have very high electrical conductivity of approximately 10^6 S/cm at room temperature (McEuen and Park 2004), a value well higher than that of metals, such as copper, at room temperature. In SWCNT films, conductivity origins from the carrier transport along the cylindrical sidewall and the carrier hopping from one tube to another and can be interpreted in the percolation theory framework (Hu *et al.* 2004). So, in principle, conductivity should increase with nanotube density. However, this is not the only parameter to take into account when the electrical performances of a carbon nanotube film are considered. As a matter of facts, the presence in the 2D or 3D random network of both semiconducting and metallic nanotubes (forming several metal-metal, semiconducting-semiconducting and metal-semiconducting junctions) as well as the tube sensitivity to chemical doping (Jackson *et al.* 2008, Zhang *et al.* 2009, Zhou *et al.* 2005) play fundamental roles and make the transport mechanism in such mats very complex. In particular, the tunneling barrier at the junction of two semiconducting and, at a lower extent, of two metallic tubes has been reported to favor the charge carrier percolation (Hu *et al.* 2004), thus suggesting that to increase the electrical conductivity it is necessary to fabricate SWCNT films with a high percentage of semiconducting (or metallic) nanotubes. In addition, the electrical conductivity can be significantly increased due to the set-up of charge transfer process between the tubes and the dopants, though the doping effects produced on metallic or semiconducting SWCNTs have been shown to be different (Tey *et al.* 2012). Therefore, getting a highly conductive SWCNT network necessarily requires a chirality sorting process since, naturally, SWCNTs are characterized by many chiralities. Moreover, structural defects and SWCNT tendency to self-assemble in bundles are other limiting factors of the nanotube and CNT network conductivity. As far as $e-h$ pair separation regards, ideal structurally perfect SWCNTs possess no junction where excitons can be splitted. The optoelectronic effects on individual carbon nanotubes were often due to the presence of a $p-n$ junction obtained with various physical realizations: e.g., electrostatically defined (Freitag *et al.* 2003, Misewich *et al.* 2003, Lee 2005) or modulated chemical doping (Zhou *et al.* 2000). On the other side, it is well known that real nanotubes can present structural defects, kinks, twisting and bending or are organized in networks where two or more CNTs intersect so giving rise to local unconventional $p-n$ or Schottky (i.e., metal-semiconductor) junctions (Castrucci *et al.* 2004, Stewart and Leonard 2004, Furher *et al.* 2000) which may act as exciton splitters. Nonetheless, it has been demonstrated that, for carbon nanotube networks, either self-standing or deposited on an insulating substrate (e.g., glass, ...), the driving force of the $e-h$ pair separation are the Schottky

junctions formed at the metal electrode/nanotube film contacts (Lien *et al.* 2006, Lu *et al.* 2006, Sun *et al.* 2006, Merchant and Marković 2008, 2009). This means that carbon nanotubes need to be suitably manipulated or associated with another material so to form efficient junctions acting as exciton separators. Among the variety of CNT combinations reported in literature, the carbon nanotube/Si heterojunction represents a good tool to further investigate nanotube network behavior upon light illumination, due to the wide knowledge of the silicon properties. Besides, carbon nanotube/Si heterojunction solar cell is the most promising in terms of power conversion efficiency currently obtained on small research cells which, when addressed the scaling-up problem, could lead to reduced fabrication costs with respect to the conventional silicon technology.

4. Carbon nanotube/Silicon solar cells

4.1 Introduction to solar cells

The solar cell is a device converting sunlight into electrical energy. Light shining on the solar cell produces both a current and a voltage to generate electric power. Normally, when light is absorbed by matter, photons promote electrons to higher energy states, but the excited electrons quickly relax to their ground state. In a photovoltaic device, there is a driving force (e.g., an electrostatic field, a difference in free energy,...) acting to pull the excited electrons into the external circuit before they can relax. The extra energy of the excited electrons generates a potential difference which drives the electrons through a load in the external circuit, where they dissipate their energy before returning to the solar cell. The effectiveness of a photovoltaic device depends on the light absorbing material and its connection with the external circuit. A variety of materials and processes can potentially satisfy the requirements for photovoltaic energy conversion, in this review we limited to semiconductor *p-n* and metal-semiconductor junctions. In such devices the semiconductor material has to be able to absorb most of the solar spectrum in a region reasonably close to the surface. When photons are absorbed by the active material, their energy is used to excite *e-h* pairs. The excited *e-h* pairs, survived to the recombination processes, are collected at the junction in the presence of electric field (applied or generated at the interface). Subsequently, the high-energy electrons are selectively extracted at one terminal while the holes are replenished from the other terminal. Ideally, there should be a one-to-one relationship between light and electric current. Practically, an important parameter measuring the cell effectiveness is the quantum efficiency (QE) or external quantum efficiency (EQE). It represents the probability that an incident photon of energy E will deliver one electron to the external circuit. Other fundamental parameters of the solar cell are evaluated from the current density - voltage (J-V) characteristic of the cell under light irradiation: the open circuit voltage (V_{OC}), the short circuit current density (J_{SC}) and the maximum power density delivered $P_{max} = J_{max} V_{max}$, as shown in Fig. 3(a). The former two are, respectively, the maximum voltage and current density the cell can develop. All these parameters allow calculating the fill factor (FF) and power conversion efficiency or efficiency (PCE or η). The fill factor is defined as the ratio $FF = P_{max} / V_{OC} J_{SC}$ and describes the “squareness” of the J-V curve (Fig. 3(a)). The efficiency of the cell is the percentage of incident light power density that actually is transformed in electric power and it is defined as the ratio between the maximum power density delivered by the cell and the incident light power density, P_s : $\eta = P_{max} / P_s$. Efficiency is therefore related to J_{SC} and V_{OC} through: $\eta = J_{SC} V_{OC} FF / P_s$.

The four quantities: V_{OC} , J_{SC} , FF and η (or PCE) are the key performance characteristics of the solar cell. In order to compare the cell operating effectiveness, these four parameters should be defined for standard illumination conditions, which can be specified as follows: an incident power density of 100 mW/cm^2 , a temperature of 25°C and an air mass AM1.5 energy spectrum. This last corresponds the standard terrestrial solar spectrum incident on a clear day upon a sun-facing 37° -tilted surface with the sun at an angle of 41.81° above the horizon. These peculiar conditions are generally reproduced in the laboratory through specific solar simulators. Electrically, the equivalent circuit of an ideal solar cell can be sketched as a current generator in parallel with a diode. However, to take into account real cell power dissipation through several paths, a series (R_s) and a parallel shunt (R_p) resistance are included on the solar cell equivalent circuit (Fig. 3(b)). R_s originates from i) the current flow through the emitter and base of the solar cell; ii) the contact resistance between the metal contact and the active material; and finally iii) the resistance of the top and rear metal electrodes. R_p is due to leakage currents forming through the cell, at the device edges and between contacts. High series and low shunt resistances reduce the fill factor (Fig. 3(c)), and as a consequence the solar cell effectiveness. When these parasitic resistances are included the equation governing the electrical behavior of the cell becomes

$$J = J_0(e^{q(V+JAR_s)/kT} - 1) + (V + J AR_s)R_p - J_{SC}$$

In addition, very often the solar cell cannot be considered an ideal diode, where all the recombination occurs via band to band or via traps located in bulk areas out of the junction area. In real solar cell, recombination does occur in other ways (e.g., Auger recombination) and in other areas (in the junction area) of the device. The ideality factor, n , is a measure of the solar cell deviation from ideality. Thus, the J-V characteristic equation, excluding the parasitic resistances, becomes

$$J = J_0(e^{q(V/nkT} - 1) - J_{SC}$$

The n value typically is between 1 and 2, being 1 the value assumed in the ideal case. Values up to 3 are also possible for p - n diodes characterized by high Auger recombination of the carriers.

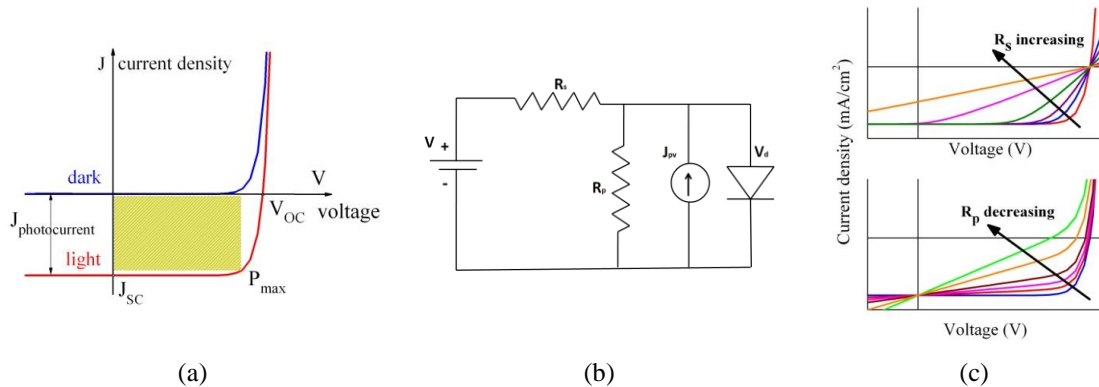


Fig. 3 (a) J-V curve for a photovoltaic device in dark and under illumination conditions. Some relevant parameters (namely the short circuit current density, J_{SC} , the open circuit voltage, V_{OC} , and the maximum power produced, P_{max}) of the solar cell are indicated; (b) solar cell equivalent circuit, (c) J-V characteristic changes as a function of R_s increasing (upper panel) and R_p lowering (lower panel)

Table 1 Summary of different CNT/crystalline Si solar cell architectures and findings as reported in literature: the cell properties

Publication details		Cell properties										
#	Reference	Active area [cm ²]	J_{SC} [mA/cm ²]	V_{OC} [V]	FF [%]	PCE [%]	R_s [Ω]	R_p [k Ω]	Rectification ratio	Ideality factor		J_0 [μ A/cm ²]
										n_1	n_2	
1	Wei <i>et al.</i> 2007	0.49	13.8	0.5	19	1.4	30-200	-	5×10^2	-	-	30
2	Jia <i>et al.</i> 2008	0.49	26.0	0.54	53	7.4	12.8	20	10^3	3.68	2.62	10.2
3	Li <i>et al.</i> 2008	0.25	21.0	0.48	28	1.3	-	-	-	-	-	-
4	Li <i>et al.</i> 2009	0.25	26.5	0.49	35	4.5	16	-	-	-	-	-
5	Jia <i>et al.</i> 2010	0.49	18.6	0.53	42	4.1	-	-	-	-	-	-
6	Ong <i>et al.</i> 2010b	0.25	14.6	0.37	30	1.7	150	7	-	3.75	-	-
7	Wadhwa <i>et al.</i> 2010	0.08	25.0	0.55	79	10.9	-	-	-	-	-	-
8	Jia <i>et al.</i> 2011a	0.09	29.0	0.56	68	10.9	66	-	1.2×10^5	1.46	-	-
9	Jia <i>et al.</i> 2011b	0.09	36.3	0.53	72	13.8	25	-	-	1.4	-	-
10	Jia <i>et al.</i> 2012	0.09	24.0	0.54	57	8.8	30-40	3×10^3	2.8×10^5	1.4	-	5×10^{-3}
11	Bai <i>et al.</i> 2012	0.09	29.3	0.55	64.4	10.3	3.3	-	-	3.1	-	-
12	Jung <i>et al.</i> 2013	-	28.6	0.53	74.1	11.2	-	-	-	1.1	-	7×10^{-5}
13	Li <i>et al.</i> 2013	0.09	29.3	0.53	73.8	11.5	-	-	-	1.08	-	2.8×10^{-3}
14	Di <i>et al.</i> 2013	0.12*	33.4	0.54	58.3	10.5	~14	-	-	~1.1	-	-
15	Shi <i>et al.</i> 2013	0.15	32.0	0.61	77	15.1	-	-	-	-	-	-

*Rectangular array of several 1×0.12 cm² windows

4.2 Carbon nanotube/Si solar cell architecture

Conventional Si solar cells have *p-n* junctions inside for an efficient extraction of light-generated charge carriers. However, the *p-n* junction is normally formed through very expensive processes requiring very high temperature ($\sim 1000^\circ\text{C}$). Therefore, there is a significant interest in forming heterojunctions at lower temperatures. In this regard, CNT networks offer an interesting and viable alternative, because of their mostly chemical, room temperature and rather cheap construction procedure. In the carbon nanotube/Si solar cells, the p-type Si layer (the so-called emitter) is replaced by a semitransparent CNT film deposited on the n-doped Si wafer, thus giving rise to an overall reduction of the total Si thickness and to the fabrication of a device with quite inexpensive methods. In particular, the CNT film works on the Si wafer as a charge carrier collecting conductive electrode and establishes a built-in voltage for separating photocarriers. Moreover, due to the CNT film optical semitransparency, most of the incoming light is absorbed in Si; thus the efficiency of the hybrid CNT/Si solar cell may in principle be comparable to a conventional Si *p-n* junction solar cell. To this aim, SWCNTs are widely used, but the performances of DWCNT/Si and MWCNT/Si photovoltaic devices have been studied too. In Tables 1, 2 and 3 are detailed the main characteristics of the CNT/Si devices reported in literature so far, at the best of our knowledge.

The first paper on carbon nanotube/Si heterojunction solar cells dates back to 2007 when Wei *et al.* (2007) demonstrated that semitransparent thin networks of DWCNTs conformally coated on an n-type Si substrate show power conversion efficiencies even higher than 1%. In the following years

Table 2 Summary of different CNT/crystalline Si solar cell architectures and findings as reported in literature: nanotube properties

Nanotubes										
#	Type	Chirality (<i>n,m</i>)	Diameter [nm]	Thickness [nm]	R_{sh} [Ω /sq]	Deposition method	Cell Treatment	T_{550} [%]	Doping	CNT film ordering
1	DWCNT	-	2-2.5	50	0.5-5	Aqueous film transfer	-	>60	-	Random
2	DWCNT	-	2	20-50	-	Aqueous film transfer	-	>60	-	Random
3	SWCNT	-	0.6-1.1	-	170	Spray-DMF*	-	69	SOCl ₂	Random
4	SWCNT	(6,5)(7,5)	-	~250	~500	Spray-DMF	-	57	SOCl ₂	Random
5	DWCNT	-	-	-	282	MCE**	-	91	-	Random
6	SWCNT	(7,6)(8,6)	0.9	-	1000	Spray-dichlorobenzene	-	83	-	Random
7	SWCNT	-	-	~45	-	MCE	Electronic control of the junction	-	-	Random
8	SWCNT	-	-	-	97	Free transfer	PDMS*** encapsulation	-	HNO ₃	Random
9	SWCNT	-	-	-	<200	Free transfer	Wet doping	>85	HNO ₃	Random
10	SWCNT	-	-	10-20	-	-	Air exposure ($T=25^{\circ}\text{C}$, humidity < 5%) for 140h	-	-	Random
11	SWCNT and DWCNT	-	0.7-3	-	300	Aqueous film transfer	-	80	A few drops of H ₂ O ₂ (0.1 % wt)	Random
12	SWCNT	-	-	-	-	Superacid sliding coating	HF+HNO ₃	>90	Gold salt	Aligned
13	SWCNT	-	-	-	-	Superacid sliding coating	HNO ₃ (0.5 mol L ⁻¹)	-	Gold salt	Aligned
14	DWCNT	-	4-6	50-100	~1700	Transfer of a spinnable nanotube array	-	~70	-	Aligned
15	SWCNT	-	-	-	-	Aqueous film transfer	TiO ₂ nanoparticle film (50-80 nm thick)	-	HNO ₃ /H ₂ O ₂ (30 % wt in water)	Random

* DMF: dimethylformamide.

** Nanotube deposition method based on vacuum filtration of the CNT dispersion onto mixed cellulose ester (MCE) membranes with subsequent removal of the MCE by dissolving in acetone.

*** PDMS: polydimethylsiloxane

Table 3 Summary of different CNT/crystalline Si solar cell architectures and findings as reported in literature: the crystalline silicon substrate properties, front and back electrode characteristics

#	Silicon				Front contact			Back contact		
	Dopant concentration [atoms/cm ³]	Resistivity [Ω cm]	Active area treatment	Thickness [μ m]	Oxide at interface [nm]	Oxide under metal [nm]	Type	Thickness [nm]	Type	Thickness [nm]
1	-	-	HF	525	-	Isinglass sheet	Ag	-	Ti/Pd/Ag	2000
2	10^{15} - 10^{16}	2-4	HF	-	-	300	-	-	Au/Ti	10
3	-	-	-	-	-	Insulator	-	-	-	-
4	-	-	-	-	-	Insulator	Ag	-	Ag	-
5	-	-	HF	-	-	-	-	-	-	-
6	-	0.01	HF	-	-	-	Ag	-	Cr/Au	20/150
7	10^{14} - 10^{15}	4-20	BOE	-	-	1000	Cr/Au	5/80	GaIn/Steel	-
8	10^{15} - 10^{16}	2-5	HF	-	-	-	-	-	Ti/Au	-
9	10^{15} - 10^{16}	2-4	HF	-	-	300	-	-	Ti/Au	-
10	-	-	-	-	-	300	-	-	Ti/Au	-
11	-	-	-	-	-	-	Ag	-	Ti/Au	-
12	10^{15} - 10^{16}	-	-	-	-	500	Cr/Au	-	Al	-
13	-	1-10	HF	-	-	-	Cr/Au	5/80	Al	-
14	-	1-10	-	-	-	Al ₂ O ₃ 400	Ag	-	GaIn	-
15	-	0.05-0.2	HF + ethanol vapors	400	-	400	Ag	~1000	GaIn	-

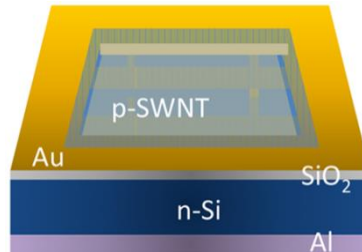


Fig. 4 Schematic of a SWNT/Si hybrid solar cell, with the surface Au electrode, a film of SiO₂ as insulator under the Au front electrode, a squared n-Si active coated by a network of SWCNTs. In this case, the metal electrode on the back is of Al. Reproduced with permission from Jung *et al.* (2013) Copyright (2013) American Chemical Society

a number of papers appeared reporting improvements to the CNT/Si solar cell giving rise to higher and higher PCEs, up to the current maximum value of 15% (Shi *et al.* 2012) and probably there is still room for further cell efficiency increase. Indeed, the characteristics and the behaviour of such a device, mainly due to the CNT network and to its interplay with the silicon substrate, have been not fully understood and deserve more studies. Up to now, several factors have been evidenced to contribute to the cell effectiveness. Although factors are often interplaying, among them most are

strictly connected to the physical properties of the materials involved, some others are more related to technical warenesses to account for in the cell design and fabrication. The simplest device investigated can be summarized (see sketch in Fig. 4) as a silicon substrate with a metallic back contact electrode and a CNT network conformally coating the Si active area and an insulator partially or totally surrounding the active area. A metal film covering the insulator generally works as the surface electrode. Seldom silver paint contacts are instead directly put on the nanotube film coating the insulator. The equivalent circuit of such devices can be schematized as the one reported in Fig. 3(b). Therefore in order to achieve the solar cell maximum efficiency, it is necessary to minimize the series resistance (R_s) and to maximize the shunt resistance (R_p). The factors contributing to these two resistances are numerous.

4.2.1 The R_s and R_{sh} contribution

As far as R_s regards, its value comes from the CNT network sheet resistance, R_{sh} ,¹ from the silicon wafer and from the front and back contact resistances as well. On the other hand, the carbon nanotube network thickness and superficial density are at the base of its sheet resistance value. However, nanotube network is a porous structure made of random distribution of small bundle or single CNTs (Fig. 5) and it is hard to define its thickness. In order to circumvent this difficulty, optical transmission is used as a good tool able to average the structural irregularities

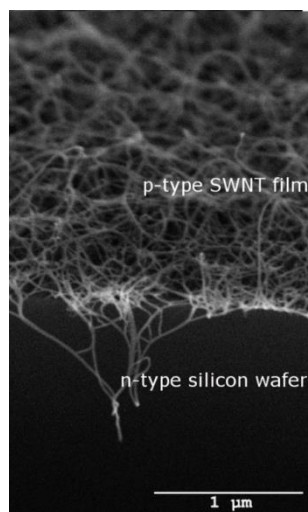


Fig. 5 SEM image of a SWCNT film showing porous network structure and the SWCNTs (individual or arranged in bundles) in close contact to the n-Si surface. Adapted with permission from Li *et al.* (2009) Copyright (2009) American Chemical Society

¹The sheet resistance, R_{sh} , measurement is used for thin films which are considered as two-dimensional entities. In this case, it is implied that the current flow is along the plane of the sheet, not perpendicular to it. The overall resistance of the film is related to R_{sh} , through the following relation: $R = R_{sh} L/W$, where current flows in the L direction and W is the other surface dimension of the film. Therefore, the units of R_{sh} are ohm. Nonetheless, generally it is reported in terms of Ω/sq or Ω/\square , so not to confuse it with bulk resistance. The reason for the name "ohms per square" is that a square sheet with sheet resistance 10 ohm/square has an actual resistance of 10 ohm, regardless of the size of the square.

and characterize the thickness of thin CNT networks² (Wei *et al.* 2007, Li *et al.* 2009). This permits to correlate optical transmittance (T) of the CNT network and its R_{sh} value (Li *et al.* 2009, Jia *et al.* 2010, Le Borgne *et al.* 2012), showing that R_{sh} decreases with T , i.e., the denser and thicker is the nanotube network, the lower is its sheet resistance. Thus, one should expect that the lowest T network presents the highest power conversion efficiency. But, this syllogism doesn't work. Indeed, Wei *et al.* (2007) reported that J_{SC} and PCE have maximum values in correspondence of an intermediate optical transparency of the DWCNT networks they were using. This finding was subsequently confirmed in other papers even for SWCNTs and MWCNTs (Li *et al.* 2009, Jia *et al.* 2010, Del Gobbo *et al.* 2011, Le Borgne *et al.* 2012, Del Gobbo *et al.* 2013) and can be interpreted as following. A reduction of the film transparency can be associated to an increase of i) the density of CNTs on the silicon surface and ii) the average thickness of the overall network. The increase of the total area covered by CNTs on the Si surface could enhance the charge carrier transport towards the surface electrodes (giving rise to R_{sh} reduction) and implies that a higher number of CNT/Si junctions are available for the separation of the photogenerated $e-h$ pairs. However, from some transmittance value on (i.e., for thicker and thicker films), more and more nanotubes are suspended on those underneath and cannot touch the Si substrate to form junctions. This means that they do not contribute to photocurrent generation and, at the same time, they absorb light thus preventing radiation from reaching the silicon substrate (where most of the $e-h$ pairs are generated). In this framework, Jia *et al.* (2010) found a correlation between the figure of merit (FM), an index used to evaluate the performances of transparent conducting films, with the PCE of CNT/Si solar cells. The FM is defined as $FM = T_{550}/R_{sh}$, where T_{550} is the optical transmittance for a photon wavelength $\lambda = 550$ nm (Haacke 1976).

As far as the effect of metal contacts on R_s regards, Wei *et al.* (2007) demonstrated that the presence of an ohmic contact at the bottom of the n -Si substrate is fundamental to get R_s reduction. They showed, indeed, that the short current density gains a factor 10 when on the n -Si back surface is deposited, instead of a silver paint film, a $2\mu\text{m}$ thick Ti/Pd/Ag layer, which has a good adhesion to silicon surface and forms an ohmic contact. In a subsequent paper, the same group increased to 7.4% the PCE of their DWCNT/ n -Si device, with J_{SC} passing from 13.8 mA/cm^2 to 26 mA/cm^2 and FF improvement from 29% to 53% (Jia *et al.* 2008). The J_{SC} gain was attributed to a slight R_s reduction probably due to an improvement of the surface and back contacts. However, other factors could have played important role: i.e., the surface electrode surrounding all the active window and the removal of native silicon oxide on the Si active area by using hydrofluoric acid. In particular, the former will allow more charge carriers, transported through the nanotube network, to reach the front metal contact and enter in the external circuit, because of the reduced path length for many of them from the generation site and the collecting electrode.

4.2.2 The presence of SiO_2 thin film at CNT/Si interface and the CNT/Si heterojunction type

The presence of a few nm thick native SiO_2 at interface between Si active region and the carbon nanotube network, instead, could be one of the origin of the kink in the J-V curve under

²Since the optical transmission of the carbon nanotube network deposited on the silicon wafer cannot be measured due to the Si thickness of the order of hundreds micrometer, generally the same CNT agglomeration is deposited both on the silicon and on a glass or quartz substrate.

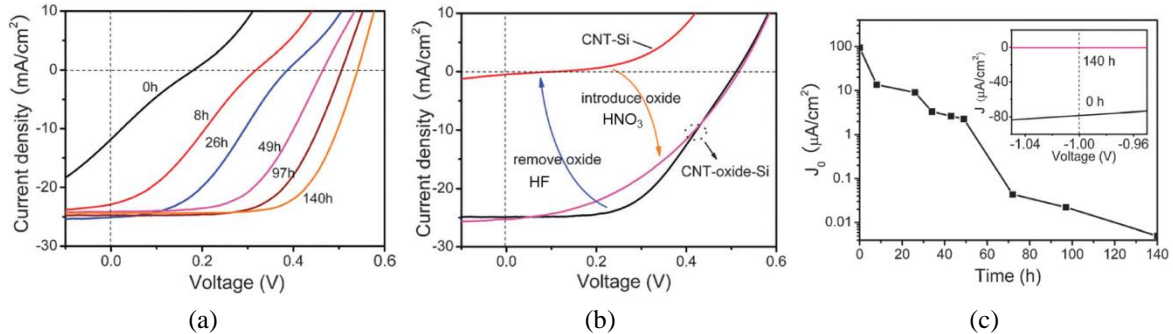


Fig. 6 (a) J-V characteristics of an optimized CNT-Si solar cell after storage in air for different periods up to 140 h. (b) J-V curves of a cell with interfacial oxide (CNT-oxide-Si), after removal of oxide by HF vapor (CNT-Si), and after reformation of the oxide layer by HNO₃ vapor. Arrows indicate each process. (c) Reverse saturation current densities (J_0), extracted from J-V characteristics acquired in dark conditions, corresponding to cells after different oxidation times. Inset, plots of reverse current density in the negative bias region (around ~ -1 V) for the fresh cell (0 h) and after 140 h storage in air. All the three figures have been adapted with permission from Jia *et al.* (2012) copyright (2012) Owner Societies

illumination (see Figs. 6(a) and (b)) and of the low resulting FF. This is clearly shown in a recent paper by Jia *et al.* (2012), who monitored the J-V characteristics of a CNT/Si solar cell for a controlled silicon oxide growth period of 140h. Fig. 6(a) shows the gradual shift of the J-V curves (recorded under standard illumination) to improved cell performances with increasing oxidation times in air at stable temperature (25°C) and humidity (5%), starting from the Si surface in a pristine state after removing the native oxide using HF. In fact, from the initial V_{OC} of 0.18 V, J_{SC} of 11.4 mA/cm², poor fill factor of 23% and a PCE of 0.5% with a pronounced kink, upon oxide growth the kink progressively disappeared and after 140h, for about 1 nm thick oxide film, the cell reached a V_{OC} of 0.54 V, a J_{SC} of 24 mA/cm², a FF of 67%, and an efficiency of 8.8%. Moreover, in the same article, the authors reported that the cell performances can be reversibly lost and gained by subsequent exposure to HF and HNO₃ vapors, removing and forming the oxide layer, respectively (Fig. 6(b)).

Similar results, have been recently confirmed by Pintossi *et al.* (2013), who performed a detailed X-ray photoelectron spectroscopy (XPS) study of the CNT/Si junction before and as a function of time from a HF vapor etching. In addition, Jia *et al.* (2012) also showed that with oxidation increasing, consistently decrease the values of the reverse current density, J_0 , (Fig. 6(c)) and the ideality factor n of the J-V characteristic acquired in dark conditions. Moreover, a study of the J-V curves in dark conditions as a function of temperature allowed the authors to suggest carrier transport mechanism occurring through a pure thermoionic model in the oxide free junction and, otherwise, through a competition of thermoionic emission and tunneling, with a decreasing proportion of thermoionic emission (a major part of J_0) with oxide layer increasing (Jia *et al.* 2012). On the other hand, the lowering of the saturation current, J_0 , can justify the larger open circuit voltage, according to the well-known relation: $V_{OC} = nkT/q \ln(J_{SC}/J_0)$. Furthermore, it was also indicated that the enhancement of the shunt resistance and the n value improvement can result from the combination of the several factors including the increase the potential barrier and passivation of the CNT/Si interface trap states, giving rise to reduction or inhibition of charge carrier recombination events (Jia *et al.* 2012, Jia *et al.* 2011a). In these and other papers (Benham

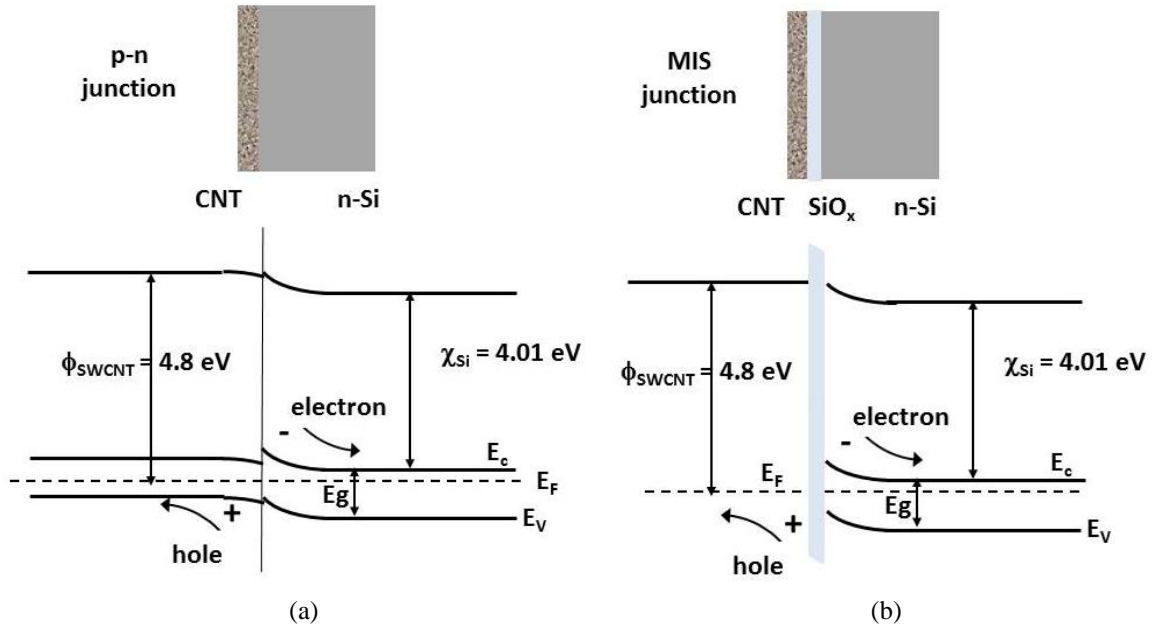


Fig. 7 Device schematics (upper panels) and energy diagrams (lower panels) for p-n (a) and MIS (b) heterojunctions. For Si are assumed an electron affinity of 4.01 eV, a band gap energy of 1.12 eV and a n-dopant concentration of about $1 \times 10^{15} \text{ cm}^{-3}$ shifting the Fermi level to about 0.25 eV below the conduction band minimum energy, E_c . Carbon nanotubes work function is assumed to be 4.8 eV. Semiconducting CNTs are assumed to have an energy gap of 0.8 eV with the nanotube Fermi level at about 0.1 eV below the middle of the bandgap due to oxygen adsorption

et al. 2008, Benham *et al.* 2010, Wadhwa *et al.* 2010), it was suggested that the SWCNT/Si junction behaves like a metal/semiconductor (MS) junction whose performances may be improved by formation of a metal/insulator/semiconductor (MIS) junction through a thin (1 nm) silicon oxide film (Jia *et al.* 2012, Jia *et al.* 2011a, Benham *et al.* 2008, Benham *et al.* 2010). In other papers, instead, the CNT/Si junction operation was interpreted as that of a p-n heterojunction (Jia *et al.* 2008, Li *et al.* 2009, Ong *et al.* 2010a, Ong *et al.* 2010b, Jung *et al.* 2013) due to the prevalent semiconducting character of the used SWCNTs (Li *et al.* 2009, Ong *et al.* 2010a, Jung *et al.* 2013). In particular, in Jung *et al.* (2013) the HNO_3 treatment of the device is not considered to create a thick enough silicon oxide film to make likely the MIS model of CNT/Si heterojunction. The mechanisms at the basis of these two main heterojunction models (namely, the p-n and MS/MIS ones) can be summarized as following. In the former, shown schematically in Fig. 7(a), nanotubes act as a p-type emitter. In this framework, i) photons are absorbed mainly in the n-Si substrate and at a lower extent in the nanotube network due to the high transparency of the CNT films generally used; ii) excitons, reaching the depletion regions without suffering recombination, are there separated by the built-in potential formed by Fermi level equilibration at the junction; iii) minority carriers are respectively drifted in the two differently doped regions thus giving rise to the photocurrent. The Schottky or the closely related MIS junction (Fig. 7(b)) mechanism, instead, can be ascribed to the metal behavior of the nanotubes. In this configuration, excitons, generated upon photon absorption, diffuse toward the depletion region (which is only in the semiconductor

side)³ where are separated by the built-in potential formed between the metal and the silicon. A large recombination of the majority carriers (electrons) passing from *n*-silicon to the metal results due to the relatively small barrier height. This gives rise to a saturation (or reverse) current typically well larger than that of a *p-n* junction diode and as a consequence of a low open circuit voltage. In this regard, the presence of an insulating thin layer is beneficial because if its conduction band energy, E_{Cox} , is well higher than that of the semiconductor, E_C , the E_C-E_{Cox} offset constitutes a large barrier, confining the electrons in silicon, which otherwise would have recombined in the metal. At the same time, instead, the electric field drives the minority carriers towards the barrier, where they can pile up to a certain degree while waiting to tunnel through. As a result, tunneling mechanism is at the base of the transport mechanism of the minority carriers through the thin insulating oxide of a MIS junction (Card 1977). Moreover, the thin insulating layer between the metal and the semiconductor may passivate interface states which are likely to trap charges increasing recombination effects and to limit the device open circuit voltage. Since the major part of the CNTs used to fabricate the cells present a variety of chiralities, it is only tempting to presume which is the dominating type of junction in the device. This distinction appears easier to be done for those devices based on chirality sorted SWCNTs as reported in Li *et al.* (2009), Ong *et al.* (2010b), and Jung *et al.* (2013). Which is the more efficient type of junction is still an open question deserving detailed studies. It has been recently addressed by Del Gobbo *et al.* (2013), who studied the effectiveness of the solar cells based either on prevailing metal nanotubes (i.e., 65%) or highly semiconducting SWCNTs (i.e., 85%). In this paper, the authors suggest that the device efficiency is strongly dependent on the sheet resistance (and therefore on the thickness and areal density) of the SWCNT networks, showing that for sheet resistances up to a certain value, the PCE is higher for the 65% metallic SWCNT/Si devices than for the semiconducting SWCNT based one while for lower R_{sh} values, semiconducting SWCNTs origin higher PCEs (Del Gobbo *et al.* 2013). In addition, the actual role of the thin oxide insulating layer is still to put in evidence and in particular if the thin oxide insulating layer is beneficial only in the Schottky barrier case, providing the formation of a MIS junction (Jia *et al.* 2012, Jia *et al.* 2011a, Benham *et al.* 2008, Benham *et al.* 2010) or serves also to improve the *p-n* heterojunction behaviour. The major part of these studies are based on the observations of tunneling transport mechanism in such devices. However, it is worth noting that tunneling transport can be found also in thin layer *p-n* heterojunctions (Ribben and Feucht 1966, Zeidenbergs and Anderson 1967, Anderson 1962) and, in particular, it has been found to play an important role in a *p*-type SWCNT/*n*-GaAs heterojunction (Liang and Roth 2008), thus pointing out that this kind of transport mechanism is not a peculiarity of MIS junctions. Besides, the beneficial effects on V_{OC} , J_{SC} and FF of a suitably thin SiO₂ film have been recently reported by Pintossi *et al.* (2013) on a CNT/Si device with the 85% of semiconducting SWCNTs. From this small review of the experimental findings and their interpretation, it is clear that the CNT/Si heterojunction based

³In the case of carbon nanotubes / silicon heterojunction, the formation of the inversion layer at the interface should be not likely. Indeed, it depends on the energy levels of the materials involved in the junction. In particular, a depletion layer is present when, with respect to the vacuum energy, the energy valence band of the semiconductor, E_V , is lower than the Fermi energy of the metal, E_{Fm} , and both are lower than the Fermi energy of the semiconductor, E_{Fs} ; otherwise if $E_{Fm} < E_V < E_{Fs}$ an inversion layer is formed. Though a wide range of work function has been attributed to CNTs (from 4.8 to 5.1 eV), Si E_V (which is equal to the Si energy gap, E_g (1.12 eV) summed to the Si electron affinity, χ (4.01 eV) (Grosso and Pastori Parravicini 2000)) is about 5.13 eV, so that $E_{Fm} < E_V$.

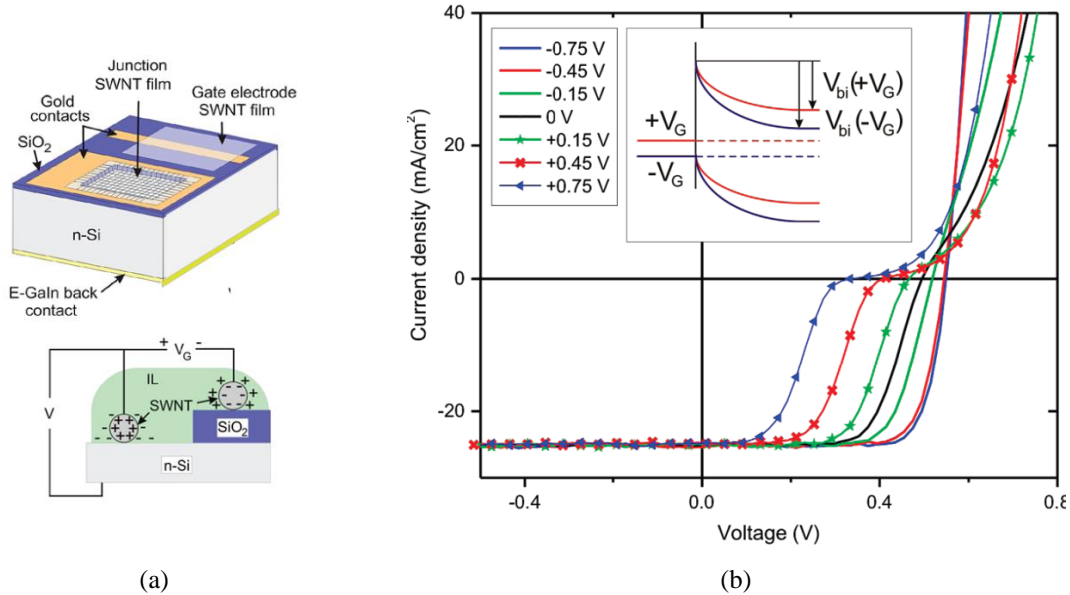


Fig. 8 (a) Schematic of the electrically-gated solar cell (upper panel) and of charge distribution during gate operation (lower panel). (b) J-V characteristics of the illuminated SWCNT/*n*-Si device under the indicated gate voltage applied to the gate electrode. Inset shows the change in built-in potential due to more or less silicon band bending with the gate voltage. Adapted with permission from Wadhwa *et al.* (2010) copyright (2010) American Chemical Society

device is well more complex than expected and needs more sophisticated approaches to be understood. This was evidenced by Wadhwa *et al.* (2010) who suggested a method of improving the solar cell FF and V_{OC} through electronic junction control of the device by using a gate potential applied to the heterojunction via an ionic liquid electrolyte (Fig. 8). As a result, the device PCE was dynamically and reversibly changed between 4 and 11% by electronic gating. The V_{OC} variation is explained in terms of nanotube Fermi level modulation. The presence and disappearance of the kink in the fourth quadrant of the J - V curves under illumination are ascribed to gate-modulated enhancement or suppression of the interface dipole at the CNT/Si junction, respectively. Interface dipole contributes as a tunneling barrier, whose effect is folded into the heterojunction barrier height, thus increasing or decreasing the recombination losses which in turn manifest themselves as reduced or enhanced photocurrent (i.e., kink presence or not) at the same applied voltage. Simple junction models do not take into account the effects on the J - V characteristics of the surface states and interface dipole that develops between the two material forming the junction. Interface dipole was associated to the polarization of chemical bonds present at the heterojunction interface (Tung 2000) or due to charge transferred by energy equilibration between the semiconducting surface states and the corresponding image charge in the metal (for a Schottky junction case, but a similar argument can be applied also to the p - n junction) (Cowley and Sze 1965). Interestingly, a recent pump and probe experiment carried out on a CNT/Si device containing a high percentage of metallic SWCNTs (65%) is likely to confirm such an interpretation, since evidenced a hole charge transfer from Si to carbon nanotubes occurring in 2 ps (Ponzoni *et al.* 2013).

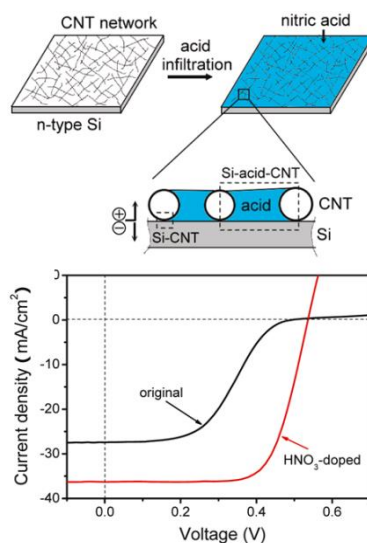


Fig. 9 Upper panel, schematic of the solar cell structure based on a CNT network coated on an *n*-type Si wafer and infiltration of nitric acid into the network to form Si-acid-CNT photoelectrochemical units in addition to Si-CNT heterojunctions at the interface. Lower panel, J-V characteristics of the solar cell before (black curve) and after (red) infiltration of dilute HNO₃. Adapted with permission from Jia *et al.* (2011b), copyright (2011) American Chemical Society

4.2.3 The SWCNT *p*-doping effect

In relation to the possibility to shift the Fermi level of the carbon nanotubes to improve the cell PCE, a number of papers explored the effect of SWCNT *p*-doping. It is worth noting, that SWCNTs, when exposed to air, naturally physisorb oxygen molecules, which origin a charge transfer making SWCNTs slightly *p*-doped (Collins *et al.* 2000). However, SWCNTs can be further external *p*-doped by chemical or substitutional methods. The former implies the interaction of SWCNTs with electron withdrawing species like strong oxidisers or oxidizing acids, the latter C atom direct substitution with *p*-type atoms like boron. At the same time, *p*-doping can increase the conductivity of the carbon nanotubes (Shin *et al.* 2009), by increasing the mobility and the number of charge carriers (holes) available at the Fermi level and therefore reducing the sheet resistance of the SWCNT network. In this framework, Saini *et al.* (2011) found through Hall measurements that substitutional B atoms in the carbon nanotube cage enhance of a factor 7 the efficiency of the solar cell owing to boron *p*-doping with very high carrier density of $1.79 \times 10^{19} \text{ cm}^{-3}$. Moreover, Li *et al.* (2008) showed that post-deposition treatment of SWCNTs with SOCl₂⁴ increases the carrier density and the effective charge carrier mobility, from 3.1×10^{15} to $4.6 \times 10^{17} \text{ cm}^{-2}$ and 0.23^5 to $1.02 \text{ cm}^2 \text{ V}^{-1} \text{ s}^{-1}$, respectively, which can be correlated to the important reduction of the carbon nanotube

⁴Experimentally the SOCl₂ was achieved by dripping three droplets of pure SOCl₂ onto the SWCNT coating film followed by drying in air. The chemical attachments of functionals to the SWCNTs are in the form of acyl chloride groups.

⁵The low mobility of the SWCNT network could be caused by several factors including high resistivity between SWCNT bundles and Schottky barriers between semiconducting and metallic nanotubes (Li *et al.* 2008) and the presence of defects due to defect action as traps for charge carrier recombination.

network resistance from 640 to 172 Ω/sq and can explain the enhancement of the measured J_{SC} and of power conversion efficiency of the cell after SOCl_2 treatment. In the same work, the authors suggested that doping, by shifting the nanotube Fermi level into the valence band, can change the electronic behavior of carbon nanotubes, promoting a switch from their semiconducting to metallic character, and therefore the mechanism of action of the SWCNT/Si heterojunctions (Li *et al.* 2008).

In 2011, Jia *et al.* (2011b) reported an increase from 6.2 to 13.8% of SWCNT/Si solar cell efficiency, by acid (HNO_3) doping of the highly porous ($\sim 70\%$, optical transmittance $> 85\%$) CNT network. In particular, they found that the PCE enhancement owed to both an improvement of J_{SC} and FF, passing from 27 to 36 mA cm^{-2} and from 0.47 to 0.72, respectively (Fig. 9). Moreover, also the ideality factor of J - V characteristic in dark conditions decreases from 2.8 to 1.4 and series resistance dropped from 36 Ω in the pristine cell to 25 Ω . They correlated this R_s reduction (and, as a consequence, of the J_{SC} and FF improvement) to nitric acid doping of the CNT porous film, as already demonstrated by other groups reporting also on its ability of remove residual molecules (Shin *et al.* 2009, Kashela *et al.* 2010). Another factor considered to enhance short circuit current is the role played by the nitric acid at nanoscale in such highly porous CNT networks. As a matter of facts, in the pristine (and all “dry”) cells some part of the external wall of nanotubes as well as some nanotubes suspended between others may have not a direct contact with the silicon surface underneath, while in the HNO_3 infiltrated “wet” cells, the acid can bridge these nanotubes to Si and assist extraction and transport of holes from Si to the CNT film. It is therefore suggested to think to the SWCNT-acid-Si systems as many nanoscale photoelectrochemical cells connected in parallel on the same side of Si, where Si is the anode, SWCNTs are the cathode and HNO_3 acts as the electrolyte. Such an hypothesis was supported with two experiments. The former allowed to demonstrate the nitric acid behavior as an electrolyte by measuring an appreciable photocurrent produced by a Si- HNO_3 -CNT device where the CNT network was separated from Si by 300 nm of HNO_3 ; the latter by observing a similar increase of J_{SC} in a typical CNT/Si hybrid cell where the nitric acid was substituted with an aqueous solution of NaCl. In this last case, however, since NaCl does not dope or/and reduce the series resistance of the nanotubes, no FF enhancement was obtained (Jia *et al.* 2011b). In addition, it is worth commenting that with respect to HNO_3 , NaCl has another inconvenient. It does not give rise to silicon oxidation so not forming a suitable thickness silicon oxide layer which is beneficial to the improvement of the FF and the kink removal in the J - V curves as also demonstrated for HNO_3 “wet” hybrid devices (Jia *et al.* 2011a). Following the same approach, Bai *et al.* (2012) reported the positive action of H_2O_2 infiltration on the effectiveness of SWCNT/Si solar cells owing to its role both as an electrolyte and in the formation of a thin silicon oxide layer at the SWCNT/Si interface. Very recently, other interpretations than the photoelectrochemical one were suggested to explain the larger J_{SC} measured for the “wet” solar cells over the “dry” ones (Li *et al.* 2013). In particular, three cooperating factors were considered more likely to give rise to the J_{SC} enhancement for “wet” devices. The first one is based on a set of studies of Michalak and Lewis (2002), and Michalak *et al.* (2008) showing that an aqueous acidic electrolyte can induce an inversion layer, thus originating a decrease of the surface recombination velocity. A reduction in light reflection is the second factor. This was attributed to the value of the acidic electrolyte index of refraction, which is between that of air and Si (Li *et al.* 2013). Last but not the least, they attributed the major improvement of the performances of the SWCNT/Si devices in their “wet” state to a “light concentration effect” due the hemispherical shape of the droplets formed by the aqueous acidic solution on the SWCNT network surface. Indeed, the authors reported that carbon nanotube porous

film may be hydrophobic or hydrophilic according to SWCNT preparation method. Significantly, in case of hydrophobic⁶ carbon nanotube network the J_{SC} consistently (~1.9 times) increases when a deionized water droplet is present on the SWCNT/Si window and recovers the original low values when it dries.

Very recently, gold salt (AuCl_3 in nitromethane) was used to provide p -doping effect (Li *et al.* 2013, Jung *et al.* 2013). SWCNT/Si heterojunction solar cells were investigated for several concentrations of AuCl_3 salt, which appeared to be distributed as several size nanoparticles on SWCNTs and Si. This study evidenced an overall increasing of J_{SC} and device performances improving up to 10 mM solution, while for higher concentration the cell effectiveness hugely resulted to degrade. The former behavior was interpreted owing to the increase of p -doping in SWCNT and, at a minor extent, to i) a slight increase of optical transmittance due to the absence of the S_{22} absorption due to downward shift of the Fermi level and consequently of the depletion of the second singularity in the valence band; ii) the presence of Au in the AuCl_3 nanoparticles which may suggest that optical scattering from these nanoparticles can contribute to enhance the light absorption. The reduction of the cell performances at salt concentration higher than 10 mM was attributed to shorting problems due to an excess of Au nanoparticles in intimate contact with Si (Li *et al.* 2013). The resulting optimized solar cell showed a short circuit current density of 28.6 mA/cm^2 , an open circuit voltage equal to 530.1 mV, and 74.1% as fill factor, so giving rise to a PCE of 11.2% and an ideality factor $n=1.1$ at room temperature (Jung *et al.* 2013). In this paper, the authors studied the carrier transport mechanism by employing temperature electrical characterization. A detailed series of studies of the dark forward and reverse J - V characteristics together with the measurements of the minority carrier recombination lifetime of these cells by using the reverse recovery transient method were made and were likely to indicate that the SWCNT/Si heterojunction operates as a p - n heterojunction (Jung *et al.* 2013). In particular, the analysis of dark saturation current as a function of temperature allowed the authors to obtain a thermal activation energy barrier, E_a , equal to 1.12 eV, a value which matches well with the band gap of Si. This made the authors suggest that the temperature-dependent rectifying characteristics originate from the thermally generated/activated intrinsic carriers in Si, and that Si is the light-absorbing/photocarrier generating active site in the SWNT/Si solar cells.

4.2.4 The role of the SWCNTs as photocarrier generators

The role of the SWCNT thin film to photocarrier generation is, indeed, an intriguing question. Most of the authors suggests that the SWCNT contribution to the photocarrier generation is insignificant, because of the very high transmittance (between 85 and 90%) of the carbon nanotube networks generally present in high performances solar cells. Actually, when comparing the external quantum efficiency spectrum of such devices with that of a classical Si p - n solar cell, the two spectra are very similar. However, at a closer look some relevant differences can be evidenced. In this regard, Ong *et al.* (2010b) reported that an excellent matching of the energy position (~1150 nm) of the absorption peaks of S_{11} band of their (7,6) and (8,6) chirality single walls and of a shoulder present in the corresponding normalized photocurrent spectrum (Fig. 10(a)), on the sharp drop-off of the silicon photocurrent signal. The presence of an absorption peak near the band gap of Si was also confirmed by Li *et al.* (2011), and Bai *et al.* (2012). Besides, the

⁶Hydrophobic SWCNT networks were obtained by using SWCNT dispersed with chlorosulfonic acid. In such cases, droplets of aqueous HNO_3 solution form large contact angles of 98° with the nanotube porous film.

former group evidenced an unexpected peak in the quantum efficiency spectra at a photon energy a little above the double of the energy of their SWCNT S_{22} transition, which was interpreted in terms of multiple exciton generation phenomenon (Li *et al.* 2011). Moreover, Le Borgne *et al.* (2012) showed, for the carbon nanotube/Si cells compared to the Si ones, a similar enhancement of the EQE spectrum in the near UV region, in correspondence to the raise of the π - π^* transition of carbon nanotubes. Furthermore, a detailed study of the EQE spectra as a function of the optical transmittance T_{550} (value measured at 550nm, $T_{550} < 70\%$) of the SWCNT networks used in the solar cell was reported by Del Gobbo *et al.* (2013) demonstrating that the wavelength (and the amount) of photocarriers coming from carbon nanotubes depend on the optical transparency value and therefore on the thickness and areal density of the SWCNT porous film. In particular, in correspondence to valley in the SWCNT transmittance due to optical transition S_{ii} , in the EQE spectra have been observed small maxima (Figure 10(b)). Significantly, the authors showed that a similar effect is present both for S_{ii} and M_{ii} transitions. Since M_{ii} transitions are associated to metal nanotubes this means that, despite the metallic character of the nanotubes, the photogenerated exciton has a lifetime long enough to reach the heterojunction without recombining. Similar contribution to photocurrent was also observed in case of multiwall carbon nanotubes, generally thought to be metallic, both in the near UV (El Khakani *et al.* 2009, Castrucci *et al.* 2006) and in the mid-infrared wavelength region (Ong *et al.* 2011a, Tsolov *et al.* 2007) and interpreted in terms of low density of electronic states at the Fermi energy for these graphitic-like systems allowing a longer exciton lifetime (Castrucci *et al.* 2011).

It is worth noting that Jia *et al.* (2010) investigated MWCNT/Si devices to study the effect of the sheet resistance and transmittance of the MWCNT network on the solar cell performances when compared to that of SWCNT porous films. The authors evidenced the higher effectiveness of the SWCNT films with respect to the MWCNT ones for a large range of values of the figure of merit. In particular, for the same network areal density, the MWCNT sheet resistance and optical transmittance are always higher than those measured for SWCNT film. This was, citing the authors, “attributed to three factors: (i) the intrinsic conductivity and high degree of crystallinity of SWCNTs, (ii) the strong inter-bundle contacts as SWCNTs form network, (iii) the volume density difference between SWCNTs and MWCNTs, i.e., SWCNT mats have a relatively lower volume density, leading to a high surface coverage on the substrate” (Jia *et al.* 2010).

4.2.5 The role of the areal density of the CNT film

The fundamental role played by the areal density was evidenced by Li *et al.* (2013) and Di *et al.* (2013) who succeeded in fabricating a highly smooth and dense SWCNT network to maximize the effective CNT/Si heterojunctions, though by following two different methods. In such a way, in fact, the authors succeeded in avoiding the SWCNT overlap and suspension on each other without contacting the Si surface leading also to a reduction of the effective distance that e - h pairs need to travel along the Si surface to meet the heterojunction where being separated and collected and of high surface recombination at the bare exposed silicon surface. In Fig. 11, the comparison of the J - V characteristics under illumination is illustrated for CNT/Si solar cells based on a random and an aligned carbon nanotube networks with the same optical transparency at 550 nm photon wavelength and the same sheet resistance. Moreover, an increase of direct charge-transfer paths, enhancing the charge collection efficiency, was suggested to be provided not only by CNT alignment but also by their long length (a few hundred of microns). In this way, Di *et al.* (2013) significantly obtained a PCE as high as 10.5% without any particular chemical treatment of the CNT/Si hybrid device.

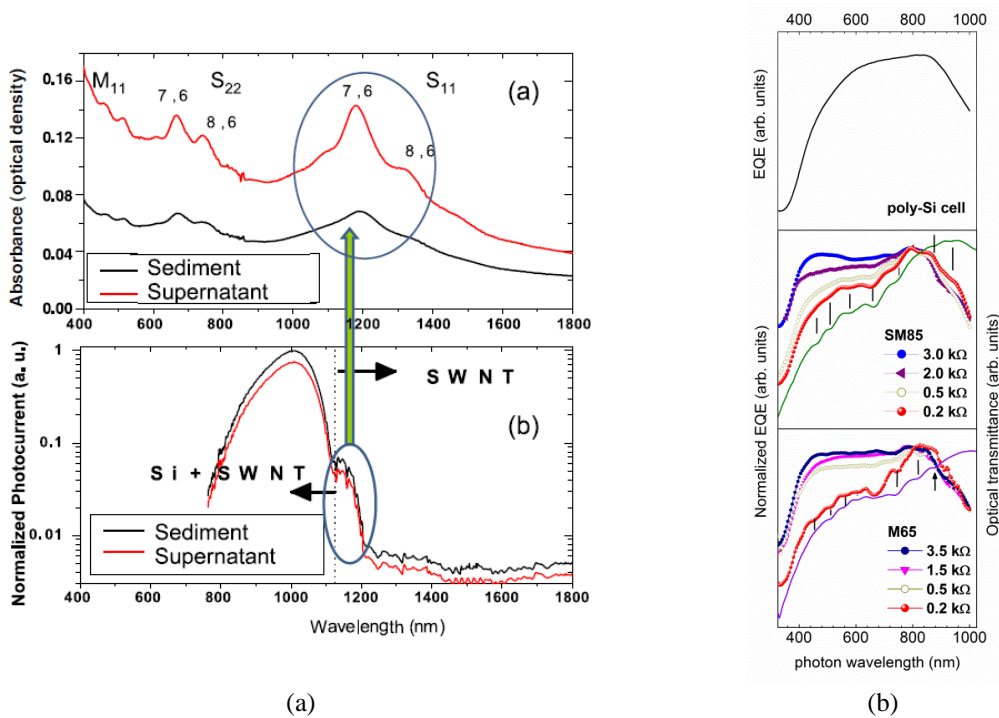


Fig. 10 (a) Upper panel, Vis-NIR absorbance spectra of SWCNT networks deposited on glass; lower panel, normalized photocurrent spectral response indicating the presence of a current peak at photon wavelength corresponding to SWCNT S_{11} transitions. Reproduced with permission from Ong *et al.* (2010b), Copyright (2010) IOP science. (b) EQE of poly-crystalline Si solar cell (upper panel), semiconducting SWCNT/Si solar cell (middle panel) and metallic SWCNT/Si solar cell (lower panel). Comparison with normalized optical transmittance spectra of semiconducting (dark green curve) in the middle panel and metallic (violet curve) in the lower panel. Reproduced with permission from Del Gobbo *et al.* (2013), Copyright (2013) The Royal Society of Chemistry

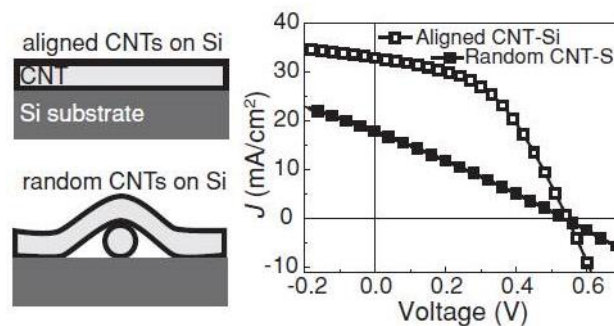


Fig. 11 Left panel, schematic showing the possible contact conditions of CNT with the silicon substrate underneath; right panel, J - V curves under illumination for CNT/Si solar cells fabricated by aligned (empty square) and random (filled square) carbon nanotube networks both characterized by the same optical transmittance at a photon wavelength of 550 nm and sheet resistance. Note the important changes in the short circuit current and fill factor. Reproduced with permission from Di *et al.* (2013), Copyright (2013) John Wiley and Sons

4.2.6 Other strategies to improve SWCNT/Si device performances

Some papers explored the possibility to improve the SWCNT/Si solar cell performances by using nanoparticles of other materials. In particular, Wang *et al.* (2012) showed that depositing a layer of CuI nanoparticles at the interface between Si and carbon nanotubes improves the short circuit current and the fill factor, giving rise to a PCE enhancement of about 20%. Moreover, also the EQE was increased upon CuI insertion. Copper iodide is a *p*-type semiconductor with a good electrical conductivity, whose high ability to transport and collect holes was suggested to be at the base of such improved performances of the solar cell. Another promising research based on the exploitation of nanoparticle properties was reported by Chen *et al.* (2013). In this paper, the authors showed that the PCE and the EQE of SWCNT/Si solar cell are significantly improved by Ag nanoparticles decorating the carbon nanotubes. This efficiency enhancement, mainly due to the J_{SC} increase, was attributed to a combination of factors, all leading to the promotion of incident light absorption. Going into details: i) the resonant interaction between the electromagnetic field of the incident light and the surface charge of metallic nanoparticles causes an electric field enhancement close to the nanoparticles which in turn gives rise to an increase of the light harvesting ability of the active layer around them; ii) the incident light can be reflected and scattered by the metal nanoparticles while passing through the active layer, thereby increasing its optical path length and improving its absorption probability. The ability of metallic (Au, Ag and Cu) nanoparticles to improve the EQE of carbon nanotube based photoelectrochemical solar cells was also demonstrated in other papers (Scarselli *et al.* 2009, Scarselli *et al.* 2011, Scarselli *et al.* 2012b) but there interpreted in terms of charge transfer enhancing the total number of carriers. Photovoltaic properties of CNT-Si solar cells were also shown to be improved by including some graphene ‘patches’ in the nanotube network (Li *et al.* 2010a) or by exposing the nanotube surface to gas flow, thus lowering the CNT network sheet resistance (Fan *et al.* 2012).

Recently, Shi *et al.* (2012) reported on CNT-Si junction solar cells with efficiencies reaching 15% by coating a TiO₂ antireflection layer and doping CNTs with H₂O₂ and HNO₃. The TiO₂ layer was deposited by spin coating and the steps followed to obtain the device are illustrated in Figure 12(a). The TiO₂ film, with thickness between 50 and 80 nm, was shown to significantly reduce light reflectance to 10% from the Si surface, to enhance the short-circuit current (by 30%) and the external quantum efficiency by nearly 90% in the visible wavelength region, but not to act on FF and V_{OC} (Figs. 12(b) and (c)). Only after the cells were treated with H₂O₂ and HNO₃ vapors, the fill factor increased up to 74% and the power conversion efficiency to 14.5% (Fig. 12(c)). The authors underlined the importance of using hydrogen peroxide vapors to reach such a good device performances due to their generation of oxygen bubbles which were likely to produce tiny pores or cracks in the TiO₂ layer making it easier for HNO₃ vapor to penetrate through TiO₂ and reach the CNT film.

4.2.7 Study of the time stability of the device

Stability over time of solar cells is one of the fundamental prerequisite of this type of devices. Shi *et al.* (2012) a consistent decrease of the fill factor in 146h (Fig. 12(d)), attributing this to the vanishing effect of the HNO₃/H₂O₂ treatment. Actually, after a new vapor exposure, the cells were reported to recover their FF value and their previous *J-V* curve shape (Fig. 12(d)). Nonetheless, the action of air exposure can lead to the cell performances degradation also because of the formation of silicon oxide (thicker than 1nm) at the CNT/Si interface. To slow down this further oxidation process, Jia *et al.* (2011a) provided the encapsulation of the active area through a transparent insulating polymer polydimethylsiloxane (PDMS). As a result, not only device stability was

greatly improved but also a slight increase of device efficiency was obtained (Fig. 13(a)). This last effect was attributed to PDMS ability to reduce reflectance from 34-40% for silicon and silicon-SWCNT to 10%. Moreover, a slight reduction in the cell performances was reported to occur in 20 day period (Fig. 13(b)) and this observation was correlated to the not complete efficiency of the PDMS encapsulation to totally suppress silicon oxide growth.

4.2.8 Other Si-based CNT/Si solar cells

Even if the major part of the research and of the promises concerns the devices based on SWCNTs and crystalline Si, the possibility to deposit carbon nanotube networks on other silicon based materials (including amorphous Si and silicon nanowires) has been also explored. As far as amorphous Si regards, at the best of our knowledge, the first report dates back to 2009 when Zhou

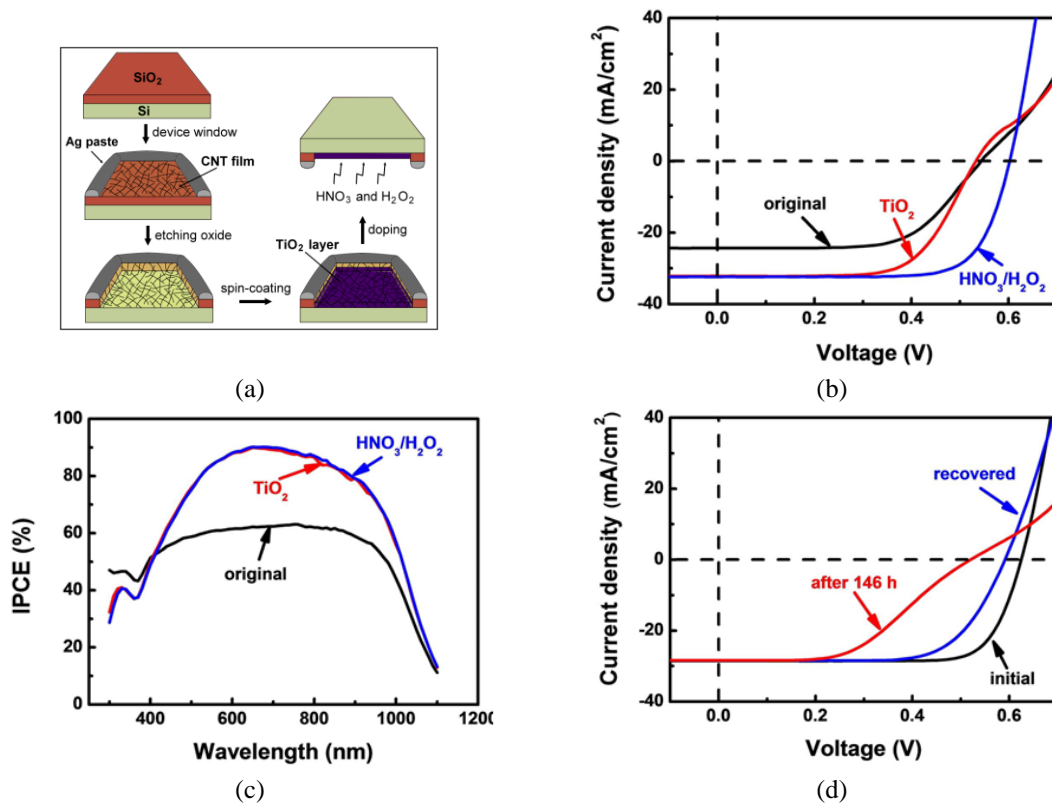


Fig. 12 (a) Illustration of the fabrication process of a TiO₂-CNT-Si solar cell involving the following steps: 1) creating a cell device window by transferring a CNT film on a Si wafer (with 400 nm oxide) and applying Ag paste around the film, 2) etching away the oxide layer to form direct CNT-Si contact and junction, 3) spin-coating a thin TiO₂ colloid on top of the CNT film as antireflection layer, and 4) chemical doping of the cell by vapor of HNO₃ and H₂O₂. (b) J-V curves of a CNT-Si cell recorded in original state (without coating), with a TiO₂ antireflection layer, and after HNO₃/H₂O₂ treatment. (c) Quantum efficiency data of the same cell in original state, with a TiO₂ layer, and after doping. (d) J-V curves of a TiO₂-CNT-Si cell measured in initial state (maximum efficiency), after storing 146 hours in air without encapsulation, and recovered by chemical doping again. Adapted with permission from Shi *et al.* (2012), copyright (2012) Nature

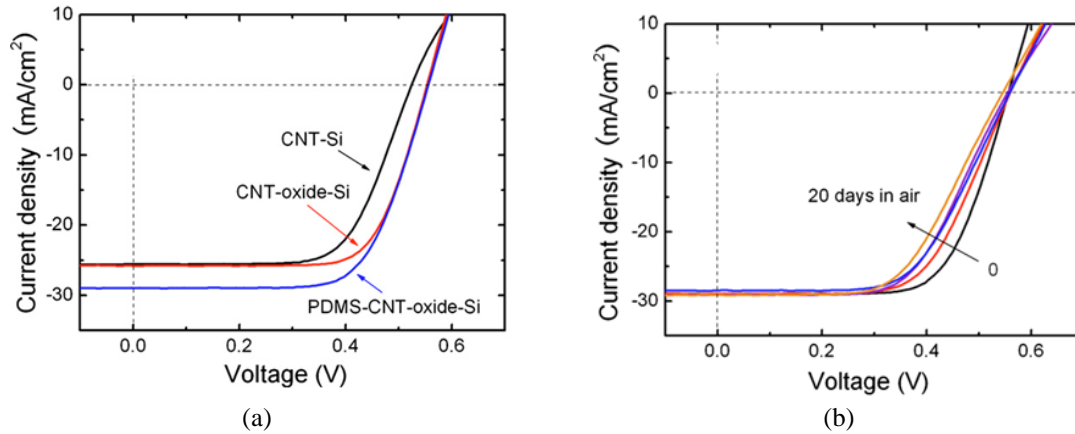


Fig. 13 (a) Light J - V characteristics of the cell at different fabrication steps. (b) J - V curves of a cell encapsulated with PDMS stored in air for 20 days. Adapted with permission from Jia *et al.* (2011a), copyright (2011) American Institute of Physics

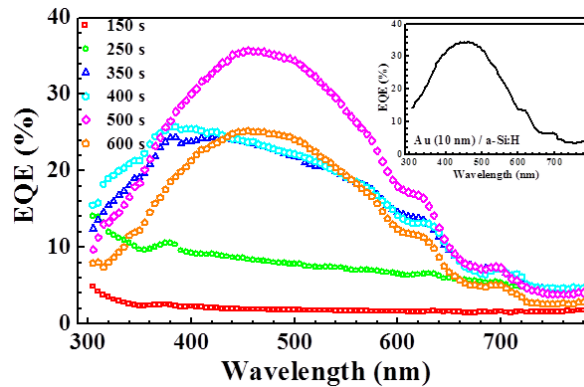


Fig. 14 External quantum efficiency spectra of SWCNT/a-Si:H devices for different spray times (in seconds, s) and therefore total amount of the carbon nanotube networks. In the inset is reported the EQE of the same characteristic a-Si:H substrate coated with an Au layer of 10 nm, in this last case the shape of the EQE corresponds to that of a-Si:H film

et al. (2009) extended the approach of fabricating solar cells with interpenetrated p - i - n or p - n junction geometry based on coaxial multishell nanowires to carbon nanotubes. In particular, the authors' strategy was based on coating vertically aligned MCWNTs grown on a tungsten coated silicon wafer with amorphous silicon (a-Si:H) shells and indium tin oxide (ITO). This device showed a 25% increase of the short-circuit current when compared to the planar a-Si cell used as reference, probably because the nanotube/nanowire arrays form a natural light-trapping structure and MCWNTs as core contacts can avoid electrical losses that might occur in other types of nanowires. A conventional planar device was proposed instead by Del Gobbo *et al.* (2011) who investigated the EQE and J - V curves behavior of SWCNT/ intrinsic a-Si solar cells as a function of the SWCNT network thickness. Significantly, the authors found that external quantum efficiency spectrum resembles that carbon nanotube optical absorption for very thin films, becoming more and more similar to that of the amorphous silicon for thicker SWCNT networks (Fig. 14). This

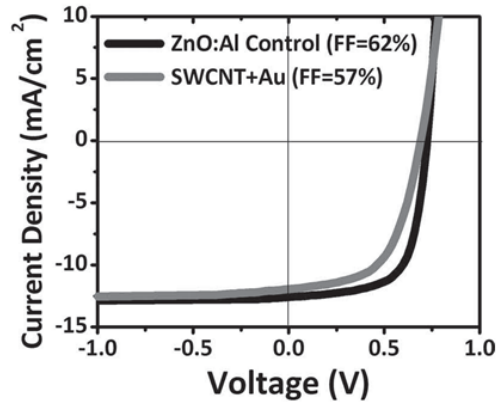


Fig. 15 J - V curves of a-Si:H solar cells with SWCNTs with Au nanodots at the p^+ /SWCNT interface and a-Si:H solar cells with ZnO:Al (and without SWCNTs) as a control sample. Adapted with permission from Kim *et al.* (2012), copyright (2012) John Wiley and Sons

result demonstrates the SWCNT ability to generate photocurrent on all the spectral range. In addition, J_{SC} was found to show a maximum for a carbon nanotube mat thickness peculiar value. Subsequently, Kim *et al.* (2012) reported that successful application of SWCNTs as transparent conductive electrode on a-Si:H cells requires utilization of Au nanodots in conjunction with SWCNT network coating a p^+ a-Si:H for ohmic contacts. They showed that this approach leads to achieving a respectable FF of 58% which is nearly comparable to the FF of 62% obtained from a control sample with ZnO:Al, a conventional transparent conductive oxide (Fig. 15). Further research and design on such carbon nanotube/a-Si:H devices are to be hoped because the thinness of both carbon nanotube network and amorphous silicon layers used can allow to develop flexible solar cells with very interesting efficiencies and costs.

Another collateral branch of investigations concerns solar cells based on carbon nanotubes and Si nanowires combined (Kalita *et al.* 2009) or not (Shu *et al.* 2009, Shu *et al.* 2010) with photoactive polymers. In this regard, particularly promising appeared the devices behaving at the same time as hybrid photoelectrochemistry and heterojunction solar cells with PCE reaching values up to 6%. In these cells, a carbon nanotube network was deposited on a carpet of Si nanowires among which was dispersed an electrolyte. Since Si nanowire arrays could be fabricated with low-cost methods without the utilization of Si wafers, such as a vapor–liquid–solid technique (Lombardi *et al.* 2006, Shimizu *et al.* 2007) or etching silicon thin film on glass (Sivakov *et al.* 2009), this approach could lead to interesting cost reductions.

4.2.9 Graphene/Si solar cells

At this point, it is evident that carbon nanotube network is necessary to form the heterojunction where e - h pairs are separated and act as semitransparent conducting front electrode. Graphene layer was reported to behave similarly on an n -Si substrate. For this reason, in this review some space has been addressed to illustrate interesting results reported in this field. Some years ago, Li *et al.* (2010) showed that graphene sheets on n -Si wafer form Schottky junctions and reach efficiencies up to 1.5%. In the same article, several advantages of graphene with respect of SWCNT networks were enumerated, making it promising for potential applications: i) graphene is a metal and does not present different electronic behaviors giving rise to two possible types of heterojunctions

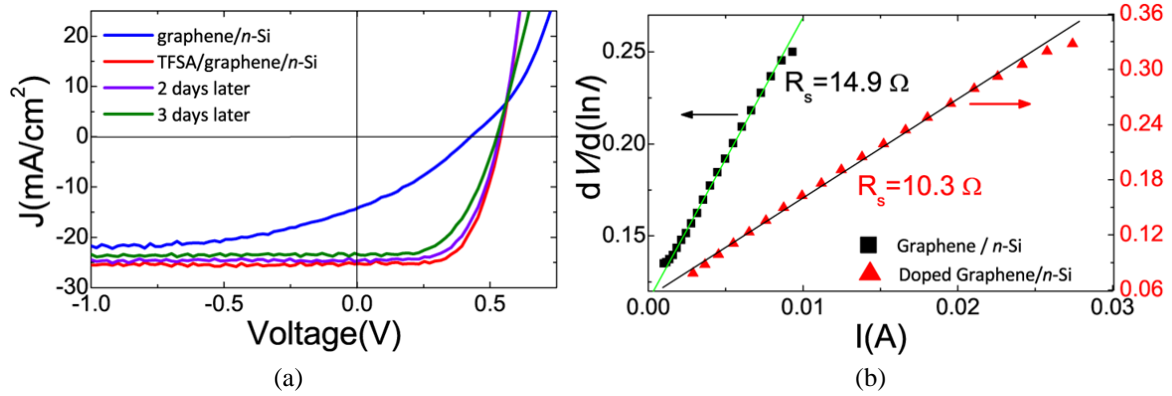


Fig. 16 (a) J - V plots of graphene/n-Si and doped-graphene/n-Si junctions under illumination with time. (b) The series resistance R_s values extrapolated from $dV/d(\ln I)$ vs I curves before and after the doping. Adapted with permission from Miao *et al.* (2012), copyright (2012) American Chemical Society

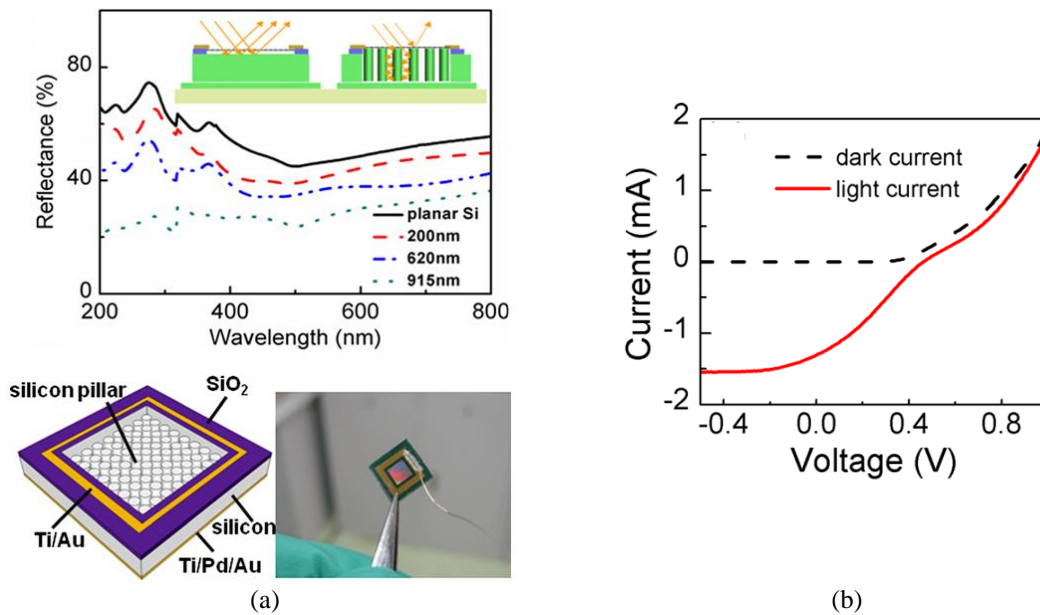


Fig. 17 (a) Upper panel, the reflectance of device with various pillar height as well as planar silicon substrate. Inset shows the principle of antireflective effect of the Si pillar substrate; lower panel, left: schematic view of a graphene/Si pillar Schottky solar cell; lower right panel: photograph of a graphene/Si pillar solar cell with 0.09 cm² junction area. (b) The I - V curves of one typical graphene/Si pillar solar cell in dark and under illumination. Reproduced with permission from Feng *et al.* (2011), Copyright (2011) American Institute of Physics

(Schottky and p - n), ii) often CNT networks exhibit a lot of interspace between bundles/tubes, which is advantageous to the transparency but sacrifices the conductivity of the film. Instead, the graphene film coating the silicon substrate is highly transparent and is formed by a patchwork of multiple layers of graphene sheets, overlapped and interconnected, ensuring a conducting pathway even if there are cracks formed in one of the layers. Similarly to carbon nanotubes, also graphene

layer doping was explored. As an example, Shi *et al.* (2010) used AuCl_3 solution to this aim, exhibiting that work function of the graphene film can varied of a value up to 0.5 eV. Their best PCE was lower than 1%. A great improvement in the graphene/Si solar cell performances was achieved by doping graphene with bis(trifluoromethanesulfonyl)-amide (TSFA) (Miao *et al.* 2012). The undoped device efficiency of 1.9% jumped to 8.6% upon TSFA doping. *J-V*, capacitance-voltage and EQE measurements indicated that the enhancement is due to the doping-induced shift of graphene chemical potential that increases the graphene carrier density and the cell built-in potential leading to reduction of the cell series resistance and increase of the cell V_{OC} , respectively (Fig. 16). Moreover TSFA dopant can be easily deposited by spin-casting and is reported to have a great environmental stability due to its hydrophobic nature. Also in the case of graphene, its combination with silicon nanostructure to form solar cells is an interesting topic to address. As an example, Feng *et al.* (2011) studied solar cells fabricated by depositing graphene on a pillar-array-patterned silicon substrate (Fig. 17) obtained by photolithography and inductive couple plasma etching. Such patterned substrate exhibited an anti-reflective characteristic and led to an absorption enhancement of the solar cell, which showed enhanced performances with respect to planar Si based devices. Moreover, the authors further improved the solar cell effectiveness with a maximum PCE of 3.55% by nitric acid treatment of the device. This was interpreted as due to the *p*-type chemical doping effect of HNO_3 which increases the work function and the carrier density of graphene.

5. Conclusions

Carbon nanotube extraordinary electronic and optical properties made them a model system for the study of a number of phenomena at nanoscale as well as a promising building block material for many different types of devices. This review is largely dedicated to CNT incorporation into future low cost Si based solar cells. In most of these devices, carbon nanotube network mainly was reported to operate as the emitter of a conventional *p-n* Si solar cell, so playing a fundamental role as *e-h* pair separator as well as transparent and conducting front electrode. During the last few years, the power conversion efficiency of these photovoltaic devices increased from about 1% of the first reports up to about 10-15%. Several methods were reported to achieve such a high PCE, among them the most used are: i) post-treatment doping of carbon nanotube networks able to lower the film resistivity and suitably shift the nanotube Fermi level; ii) formation of a thin (~1 nm) silicon oxide layer to passivate the interface states, which are likely to trap charges increasing recombination effects, and to limit the device open circuit voltage; iii) use of ionic electrolytes to provide electronic junction control; iv) alignment and use of long length carbon nanotubes to lower CNT network resistivity, maximize the number of CNT/Si heterojunctions, minimize the Si surface recombination and *e-h* pair travel distance to reach the heterojunction; v) use of antireflective TiO_2 films. The rapidity of this great improvement in the CNT/Si performances was extraordinary, also considering the low number of scientists working in this field. However, some scientific issues are far to be clearly understood. In particular, among open questions can be enumerated: i) the nature of the CNT/Si heterojunction due to the mixed chirality of the carbon nanotube used to fabricate most of the investigated devices, ii) the photocurrent generation ability of CNTs and possibility to exploit it to enlarge the EQE radiation range of the fabricated solar cell. In parallel, photovoltaic devices based on graphene/Si or CNT/a-Si:H as well as CNT/Si nanowires were reported to be promising. All this means that it is likely that further improvements

of the effectiveness of these photovoltaic devices will come in the next future. In addition, since a PCE around 15% is not far from the value of commercial Si solar cells, stability over time and larger area will be key points to be addressed in view of their possible introduction in the market.

Acknowledgments

The author wish to thank Kasher, Mirella, Cristiano and Marzia for their continuous and precious Support. The author gratefully acknowledges Prof. Maurizio De Crescenzi and Prof. Manuela Scarselli from the University of Roma Tor Vergata for helpful discussions.

References

- Akai, Y. and Saito, S. (2005), "Electronic structure, energetics and geometric structure of carbon nanotubes: A density-functional study", *Physica E*, **29**, 555-559
- American Census bureau (2012), *The 2012 Statistical abstract*, World Primary Energy Consumption by Region and Type.
- Anderson, R.L. (1962), "Experiments on Ge-GaAs heterojunctions", *Solid State Electron.*, **5**, 341-344.
- Bai, X., Wang, H., Wei, J., Jia, Y., Zhu, H., Wang, K. and Wu, D. (2012), "Carbon nanotube-silicon hybrid solar cells with hydrogen peroxide doping", *Chem. Phys. Lett.*, **533**, 70-73.
- Balasubramanian, K., Fan, Y., Burghard, M., Kern, K., Friedrich, M., Wannek, U. and Mews, A. (2004), "Photoelectronic transport imaging of individual semiconducting carbon nanotubes", *Appl. Phys. Lett.*, **84**, 2400-2402.
- Barazzouk, S., Hotchandani, S., Vinodgopal, K. and Kamat, P. V. (2004) "Single-wall carbon nanotube films for photocurrent generation. a prompt response to visible-light irradiation", *J. Phys. Chem. B*, **108**, 17015-17018.
- Benham, A., Johnson, J. L., Choi, Y., Ertosun, M. G., Okyay, A. K., Kapur, P., Saraswat, K. C. and Ural, A. (2008), "Experimental characterization of single-walled carbon nanotube film-Si Schottky contacts using metal-semiconductor-metal structures", *Appl. Phys. Lett.*, **92**, 243116.
- Benham, A., Radhakrishna, N. A., Wu, Z. and Ural, A. (2010), "Electronic properties of metal-semiconductor and metal-oxide semiconductor structures composed of carbon nanotube film on silicon", *Appl. Phys. Lett.*, **97**, 233105.
- Card, H. C. (1977), "Photovoltaic properties of MIS-Schottky barriers", *Solid State Electron.*, **20**, 971-976.
- Castrucci, P., Scarselli, M., De Crescenzi, M., El Khakani, M.A., Rosei, F., Braidy, N. and Yi, J.H. (2004), "Effect of coiling on the electronic properties along single-wall carbon nanotubes", *Appl. Phys. Lett.*, **85**, 3857.
- Castrucci, P., Tombolini, F., Scarselli, M., Speiser, E., Del Gobbo, S., Richter, W., De Crescenzi, M., Diociaiuti, M., Gatto E. and Venanzi, M. (2006), "Large photocurrent generation in multiwall carbon nanotubes", *Appl. Phys. Lett.*, **89**, 253107.
- Castrucci, P., Scilletta, C., Del Gobbo, S., Scarselli, M., Camilli, L., Simeoni, M., Delley, B., Continenza, A. and De Crescenzi, M. (2011), "Light harvesting with multiwall carbon nanotube/silicon heterojunctions", *Nanotechnology*, **22**, 115701.
- Chen, J., Hamon, M.A., Hu, H., Chen, Y., Rao, A.M., Eklund, P.C. and Haddon, R.C. (1998), "Solution properties of single-walled carbon nanotubes", *Science*, **282**, 95-98.
- Chen, L., Zhang, S., Changm L., Zeng, L., Yu, X., Zhao, J., Zhao, S., Xu, C. (2013), "Photovoltaic conversion enhancement of single wall carbon-Si heterojunction solar cell decorated with Ag nanoparticles", *Electrochem. Acta*, **93**, 293-300.
- Collins, P.G., Bradley, K., Ishigami, M. and Zettl, A. (2000), "Extreme oxygen sensitivity of electronic properties of carbon nanotubes", *Science*, **287**, 1801-1804.

- Cowley, A.M. and Sze, S. M. (1965), "Surface states and barrier height of metal-semiconductor systems", *J. Appl. Phys.*, **36**, 3212-3220.
- Del Gobbo, S., Castrucci, P., Scarselli, M., Camilli, L., De Crescenzi, M., Mariucci, L., Valletta, A., Minotti, A. and Fortunato, G. (2011), "Carbon nanotube semitransparent electrodes for amorphous silicon based photovoltaic devices", *Appl. Phys. Lett.*, **98**, 183113.
- Del Gobbo, S. Castrucci, P., Fedele, S., Riele, L., Convertino, A., Morbidoni, M., De Nicola, F., Scarselli, M., Camilli, L. and De Crescenzi, M. (2013), "Silicon spectral response extension through single wall carbon nanotubes in hybrid solar cells", *J. Mater. Chem. C*, **1**, 6752-6758.
- Di, J., Yong, Z., Zheng, X., Sun, B. and Li, B. (2013), "Aligned carbon nanotubes for high efficiency Schottky solar cells", *Small*, **9**, 1367-1372.
- Dresselhaus, M.S., Dresselhaus, G., Sugihara, K., Spain, I.L. and Goldberg, H.A. (1988), "Graphite fibers and filaments", *Springer Ser. Mater. Sci.*, **5**, Springer, Berlin.
- Dresselhaus, M.S., Dresselhaus, G. and Eklund P. (1996), *Science of Fullerenes and Carbon Nanotubes*, Academic Press, San Diego.
- El Khakani, M.A., Le Borgne, V., Aissa, B., Rosei, F., Scilletta, C., Speiser, E., Scarselli, M., Castrucci, P. and De Crescenzi, M. (2009), "Photocurrent generation in random networks of multiwall-carbon nanotubes grown by an "all-laser" process", *Appl. Phys. Lett.*, **95**, 083114.
- European Energy Council (2006), *Renewable Energy Scenario To 2040: Half Of The Global Energy Supply From Renewables In 2040*, European Renewable Energy Council.
- Fan, G., Fan, L., Li, Z., Bai, X., Mulligan, S., Jia, Y., Wang, K., Wei, J., Cao, A., Wu, D., Wei, B. and Zhu, J. (2012), "Hybrid effect of gas flow and light excitation in carbon/silicon Schottky solar cells", *J. Mater. Chem.*, **22**, 3330-3334.
- Fanchini, G., Unalan H. E. and Chhowalla, M. (2006), "Optoelectronic properties of transparent and conducting single-wall carbon nanotube thin films", *Appl. Phys. Lett.*, **88**, 191919.
- Feng, T., Xie, D., Lin, Y., Zang, Y., Ren, T., Song, R., Zhao, H., Tian, H., Li, X., Zhu, H. and Liu, L. (2011), "Graphene based Schottky junction solar cells on patterned silicon-pillar-array substrate", *Appl. Phys. Lett.*, **99**, 233505.
- Freitag, M., Martin, Y., Misewich, J.A., Martel, R. and Avouris, Ph. (2003), "Photoconductivity of single carbon nanotubes", *Nano Lett.*, **3**, 1067-1071.
- Fujiwara, A., Matsuoka, Y., Suematsu, H., Ogawa, N., Miyano, K., Kataura, H., Maniwa, Y., Suzuki, S. and Achiba, Y. (2001), "Photoconductivity in semiconducting single-walled carbon nanotubes", *Jpn. J. Appl. Phys.*, **40**, L1229-L1231.
- Fuhrer, M.S., Nygård, J., Shih, L., Forero, M., Yoon, Y.G., Mazzone, M.S.C., Choi, H.J., Ihm, J., Steven, M., Louie, G., Zettl, A. and McEuen, P.L. (2000), "Crossed nanotube junction", *Science*, **288**, 494-497.
- Gabor, N.M., Zhong, Z., Bosnick, K., Park, J. and McEuen, P.L. (2009), "Extremely efficient multiple electron-hole pair generation in carbon nanotube photodiodes", *Science*, **325**, 1367-1371.
- Galimberti, G., Ponzoni, S., Cartella, A., Cole, M.T., Hofmann, S., Cepek, C., Ferrini, G. and Pagliara, S. (2013), "Probing the electronic structure of multi-walled carbon nanotubes by transient optical transmittivity", *Carbon*, **57**, 50-58.
- Green, M.A., Emery, K., Hishikawa, Y., Warta, W. and Dunlop, E.D. (2012), "Solar cell efficiency tables (version 39)", *Progress in photovoltaics: Research and Applications*, **20**, 12-20.
- Grosso, G. and Pastori Parravicini, G. (2000), *Solid State Physics*, Academic Press, San Diego, CA, USA.
- Haacke, G. (1976), "New figure of merit for transparent conductors", *J. Appl. Phys.*, **47**, 4086-4089.
- Hamada, N., Sawada, S. and Oshiyama, A. (1992), "New one-dimensional conductors: graphitic microtubules", *Phys. Rev. Lett.*, **68**, 1579-1581.
- Ho, Y.H., Chang, C.P., Shyu, F.L., Chen, R.B., Chen, S.C. and Lin, M.F. (2004), "Electronic and optical properties of double-walled armchair carbon nanotubes", *Carbon*, **42**, 3159-3167.
- Hoffert, M.I., Caldeira K., Jain, A.K., Haites, E.F., Harvey, L.D.D., Potter, S.D., Schelsinge, M.E., Schneider, S.H., Watts, R.G., Wigley, T.M.L. and Wuebbles, D.J. (1998), "Energy implications of future stabilization of atmospheric CO₂ content", *Nature*, **395**, 881-884.
- Hu, L., Hecht, D.S. and Gruner, G. (2004), "Percolation in transparent and conducting carbon nanotube

- networks”, *Nano Lett.*, **4**, 2513-2517.
- Jackson, R., Domercq, B., Jain, R., Kippelen, B. and Graham, S. (2008), “Stability of doped transparent carbon nanotube electrodes”, *Adv. Funct. Mater.*, **18**, 2548-2554.
- Jia, Y., Wei, J., Wang, K., Cao, A., Shu, Q., Gui, X., Zhu, Y., Zhuang, D., Zhang, G., Ma, B., Wang, L., Liu, W., Wang, Z., Luo, J. and Wu, D. (2008), “Nanotube-Silicon heterojunction solar cells”, *Adv. Mater.*, **20**, 4594-4598.
- Jia, Y., Li, P., Wei, J., Cao, A., Wang, K., Li, C., Zhuang, D., Zhu, H. and Wu, D. (2010), “Carbon nanotube films by filtration for nanotube-silicon heterojunction solar cells”, *Mater. Research Bull.*, **45**, 1401-1405.
- Jia, Y., Li, P., Gui, X., Wei, J., Wang, K., Zhu, H., Wu, D., Zhang, L., Cao, A. and Xu, Y. (2011a), “Encapsulated carbon nanotube-oxide-silicon solar cells with stable efficiency”, *Appl. Phys. Lett.*, **98**, 133115.
- Jia, Y., Cao, A., Bai, X., Li, Z., Zhang, L., Guo, N., Wei, J., Wang, K., Zhu, H., Wu, D. and Ajayan, P. M. (2011b), “Achieving high efficiency silicon-carbon nanotube heterojunction solar cells by acid doping”, *Nano Lett.*, **11**, 1901-1905.
- Jia, Y., Cao, A., Kang, F., Li, P., Gui, X., Zhang, L., Shi, E., Wei, J., Wang, K., Zhu, H. and Wu, D. (2012), “Strong and reversible modulation of carbon nanotube–silicon heterojunction solar cells by an interfacial oxide layer”, *Phys. Chem. Chem. Phys.*, **14**, 8391-8396.
- Jorio, A., Dresselhaus, M.S. and Dresselhaus, G. (2008) *Carbon Nanotubes: Advanced Topics in the Synthesis, Structure, Properties, and Applications*, Springer, New York.
- Jung, Y., Li, X., Rajan, N.K., Taylor, A.D. and Reed, M.A. (2013), “Record high efficiency single-walled carbon nanotube/silicon p-n junction solar cells”, *Nano Lett.*, **13**, 95-99.
- Kalita, G., Adhikari, S., Aryal, H.R., Afre, R., Soga, T., Sharon, M., Koichi, W. and Umeno, M. (2009), “Silicon nanowire array/polymer hybrid solar cell incorporating carbon nanotubes”, *J. Phys. D: Appl. Phys.*, **42**, 115104.
- Kaskela, A., Nasibulin, A.G., Timmermans, M.Y., Aitchison, B., Papadimitratos, A., Tian, Y., Zhu, Z., Jiang, H., Brown, D.P., Zakhidov, A. and Kauppinen, E.I. (2010), “Aerosol-synthesized swcnt networks with tunable conductivity and transparency by a dry transfer technique”, *Nano Lett.*, **10**, 4349-4355.
- Kataura, H., Kumazawa, Y., Maniwa, Y., Umezū, I., Suzuki, S., Ohtsuka, Y. and Achiba, Y. (1999), “Optical properties of single-wall carbon nanotubes”, *Synth. Met.*, **103**, 2555-2558.
- Kim, J., Hong, A.J., Chandra, B., Tulevski, G.S. and Sadana, D.K. (2012), “Engineering of contact resistance between transparent single-walled carbon nanotube films and a-Si:H single junction solar cells by gold nanodots”, *Adv. Mater.*, **24**, 1899-1892.
- Kim, P., Odum, T.W., Huang, J.L. and Lieber, C.M. (1999), “Electronic density of states of atomically resolved single-walled carbon nanotubes: van Hove singularities and end states”, *Phys. Rev. Lett.*, **82**, 1225-1228.
- Kwon, Y. and Tomanek, D. (1998), “Electronic and structural properties of multiwall carbon nanotubes”, *Phys. Rev. B*, **58**, R16001-R16004.
- Le Borgne, V., Gautier, L.A., Castrucci, P., Del Gobbo, S., De Crescenzi, M. and El Khakani, M.A. (2012), “Enhanced UV photoresponse of KrF-laser-synthesized single-wall carbon-nanotubes/n-silicon hybrid devices”, *Nanotechnology*, **23**, 215206.
- Lee, J.U. (2005), “Photovoltaic effect in ideal carbon nanotube diodes”, *Appl. Phys. Lett.*, **87**, 073101
- Li, C., Li, Z., Zhu, H., Wang, K., Wei, J., Li, X., Sun, P., Zhang, H. and Wu, D. (2010a), “Graphene Nano-“patches” on a carbon nanotube network for highly transparent/conductive thin film applications”, *J. Phys. Chem. C*, **114**, 14008-14012.
- Li, X., Zhu, H., Wang, K., Cao, A., Wei, J., Li, C., Jia, Y., Li, Z., Li, X. and Wu, D. (2010b), “Graphene-on-silicon Schottky junction solar cells”, *Adv. Mater.*, **22**, 2743-2748.
- Li, X., Jung, Y., Sakimoto, K., Goh, T.H., Reed, M.A. and Taylor, A.D. (2013), “Improved efficiency of smooth and aligned single walled carbon nanotube/silicon hybrid solar cells”, *Energy Environ. Sci.*, **6**, 879-887.
- Li, Y., Kodama, S., Kaneko, T. and Hatakeyama, R. (2011), “Harvesting infrared solar energy by

- semiconducting single-walled carbon nanotubes”, *Appl. Phys. Expr.*, **4**, 065101.
- Li, Z., Kunets, V.P., Saini, V., Xu, Y., Dervishi, E., Salamo, G.J., Biris, A.R. and Biris, A.S. (2008), “SOCl₂ enhanced photovoltaic conversion of single wall carbon nanotube/n-silicon heterojunctions”, *Appl. Phys. Lett.*, **93**, 243117.
- Li, Z., Kunets, V.P., Saini, V., Xu, Y., Dervishi, E., Salamo, G.J., Biris, A.R. and Biris, A.S. (2009), “Light-harvesting using high density p-type single wall carbon nanotube/n-type silicon heterojunctions”, *ACS Nano*, **3**, 1407-1414.
- Liang, C.W. and Roth, S. (2008), “Electrical and optical transport of gas/carbon nanotube heterojunctions”, *Nano Lett.*, **8**, 1809-1812.
- Lien, D.H., Hsu, W.K., Zan, H.W., Tai, N.H. and Tsai, C.H. (2006), “Photocurrent amplification at carbon nanotube-metal contacts”, *Adv. Mater.*, **18**, 98-103.
- Liu, L., Jayanthi, C.S., Tang, M., Wu, S.Y., Tomblor, T.W., Zhou, C., Alexseyev, L., Kong, J. and Dai, H. (2000), “Controllable reversibility of an sp² to sp³ transition of a single wall nanotube under the manipulation of an AFM tip: a nanoscale electromechanical switch?”, *Phys. Rev. Lett.*, **84**, 4950-4953.
- Liu, X., Pichler, T., Knupfer, M., Golden, M.S., Fink, J., Kataura, H. and Achiba, Y. (2002), “Detailed analysis of the mean diameter and diameter distribution of single-wall carbon nanotubes from their optical response”, *Phys. Rev. B*, **66**, 045411.
- Lombardi, I., Hochbaum, A.I., Yang, P.D., Carraro C. and Maboudian, R. (2006), “Synthesis of high density, size-controlled Si nanowire arrays via porous anodic alumina mask”, *Chem. Mater.*, **18**, 988-991.
- Lu, S. and Panchapakesan, B. (2006), “Photoconductivity in single wall carbon nanotube sheets”, *Nanotechnology*, **17**, 1843-1850.
- Luque, A. and Hegedus, S. (2003), *Handbook of Photovoltaic Science and Engineering*, John Wiley & Sons, 1168.
- McEuen, P.L. and Park, J.Y. (2004), “Electron transport in single-walled carbon nanotubes”, *MRS Bull.*, **29**, 272-275.
- Merchant, C.A. and Marković, N. (2008), “Effects of diffusion on photocurrent generation in single-walled carbon nanotube films”, *Appl. Phys. Lett.*, **92**, 243510.
- Merchant, C.A. and Marković, N. (2009), “The photoresponse of spray-coated and free-standing carbon nanotube films with Schottky contacts”, *Nanotechnology*, **20**, 175202.
- Miao, X., Tongay, S., Petterson, M.K., Berke, K., Rinzler, A.G., Appleton, B.R. and Hebard, A.F. (2012), “High efficiency graphene solar cells by chemical doping”, *Nano Lett.*, **12**, 2745-2750.
- Michalak, D.J. and Lewis, N.S. (2002), “Use of near-surface channel conductance and differential capacitance versus potential measurements to correlate inversion layer formation with low effective surface recombination velocities at n-Si/liquid contacts”, *Appl. Phys. Lett.*, **80**, 4458-4460.
- Michalak, D.J., Gstrein, F. and Lewis, N.S. (2008), “The role of band bending in affecting the surface recombination velocities for Si(111) in contact with aqueous acidic electrolytes”, *J. Phys. Chem. C*, **112**, 5911-5921.
- Mintmire, J.W. and White, C.T. (1995), “Electronic and structural properties of carbon nanotubes”, *Carbon*, **33**, 893-902.
- Misewich, J.A., Martel, R., Avouris, Ph., Tsang, J.C., Heinze, S. and Tersoff, J. (2003), “Electrically induced optical emission from a carbon nanotube FET”, *Science*, **300**, 783-786.
- Mohite, A., Chakraborty, S., Gopinath, P., Sumanasekera, G.U. and Alphenaar, B.W. (2005), “Displacement current detection of photoconduction in carbon nanotubes”, *Appl. Phys. Lett.*, **86**, 061114.
- Murakami, Y., Einarsson, E., Edamura, T. and Maruyama, S. (2005), “Polarization dependence of the optical absorption of single-walled carbon nanotubes”, *Phys. Rev. Lett.*, **94**, 087402.
- Odom, T.W., Huang, J.L., Kim, P. and Lieber, C.M. (1998), “Atomic structure and electronic properties of single-walled carbon nanotubes”, *Nature*, **391**, 62-64.
- Ong, P.L., Euler, W.B. and Levitsky, I.A. (2010a), “Carbon nanotube-Si diode as a detector of mid-infrared illumination”, *Appl. Phys. Lett.*, **96**, 033106.
- Ong, P.L., Euler, W.B., Levitsky, I.A. (2010b), “Hybrid solar cells based on single-walled carbon nanotubes/Si heterojunctions”, *Nanotechnology*, **21**, 105203.

- Okada, S. and Oshiyama, A. (2003), "Curvature-induced metallization of double-walled semiconducting zigzag carbon nanotubes", *Phys. Rev. Lett.*, **91**, 216801
- Pintossi, C., Salvinelli, G., Drera, G., Pagliara, S., Sangaletti, L., Del Gobbo, S., Morbidoni, M., Scarselli, M., De Crescenzi, M. and Castrucci, P. (2013) "Direct evidence of chemically inhomogeneous, nanostructured, Si-O buried interfaces and their effect on the efficiency of CNT/Si photovoltaic heterojunctions". (under Review)
- Ponzoni, S., Galimberti, G., Sangaletti, L., Castrucci, P., Del Gobbo, S., Morbidoni, M., Scarselli, M., Pagliara, S. (2013), "Interface-coupled relaxation dynamics in CNT-Si hybrid solar cells". (submitted to ACSNano)
- Riben, A.R. and Feucht, D.L. (1966), "nGe-pGaAs Heterojunctions", *Solid State Electron.*, **9**, 1055-1065.
- Saini, V., Li, Z., Bourdo, S., Kunets, V.P., Trigwell, S., Couraud, A., Rioux, J., Boyer, C., Nteziyaremye, V., Dervishi, E., Biris, A.R., Salamo, G.J., Viswanathan, T. and Biris, A.S. (2011), "Photovoltaic devices based on high density boron-doped single-walled carbon nanotube/n-Si heterojunctions", *J. Appl. Phys.*, **109**, 014321.
- Saito, R., Fujita, M., Dresselhaus, G. and Dresselhaus, M.S. (1992), "Electronic structure of chiral graphene tubules", *Appl. Phys. Lett.*, **60**, 2204.
- Saito, R., Dresselhaus, G. and Dresselhaus, M.S. (1993), "Electronic structure of double-layer graphene tubules", *J. Appl. Phys.*, **73**, 494
- Saito, S. (1997), "Carbon nanotubes for next-generation electronics devices", *Science*, **278**, 77-78.
- Salvetat, J.P., Bonard, J.M., Thomson, N.H., Kulik, A.J., Forró, L., Benoit, W. and Zuppiroli, L. (1999), "Mechanical properties of carbon nanotubes", *Appl. Phys. A*, **69**, 255-260.
- Scarselli, M., Scilletta, C., Tombolini, F., Castrucci, P., Diociaiuti, M., Casciardi, S., Gatto, E., Venanzi, M. and De Crescenzi, M. (2009), "Multiwall carbon nanotubes decorated with copper nanoparticles: effect on the photocurrent response", *J. of Phys. Chem. C*, **113**, 5860-5864.
- Scarselli, M., Castrucci, P., Camilli, L., Del Gobbo, S., Casciardi, S., Tombolini, F., Gatto, E., Venanzi, M. and De Crescenzi, M. (2011), "Influence of Cu nanoparticle size on the photo-electrochemical response from Cu-multiwall carbon nanotube composites", *Nanotechnology*, **22**, 035701.
- Scarselli, M., Castrucci, P. and De Crescenzi, M., (2012a), "Electronic and optoelectronic nano-devices based on carbon nanotubes", *J. Phys.: Condens. Matter*, **24**, 313202.
- Scarselli, M., Camilli, L., Matthes, L., Pulci, O., Castrucci, P., Gatto, E., Venanzi, M. and De Crescenzi, M. (2012b), "Photoresponse from noble metal nanoparticles-multi walled carbon nanotube composites", *Appl. Phys. Lett.*, **101**, 241113.
- Shi, Y., Kim, K.K., Reina, A., Hofmann, M., Li, L.J. and Kong, J. (2010), "Work function engineering of graphene electrode via chemical doping", *Acs Nano*, **4**, 2689-2694.
- Shi, E., Zhang, L., Li, Z., Li, P., Shang, Y., Jia, Y., Wei, J., Wang, K., Zhu, H., Wu, D., Zhang, S. and Cao, A. (2012), "TiO₂-coated carbon nanotube-silicon solar cells with efficiency of 15%", *Scientific Report*, **2**, 884.
- Shimizu, T., Xie, T., Nishikawa, J., Shingubara, S., Senz, S. and Gösele, U. (2007), "Synthesis of vertical high-density epitaxial Si(100) nanowire arrays on a Si(100) substrate using an anodic aluminum oxide template", *Adv. Mater.*, **19**, 917-920.
- Shin, D.W., Lee, J.H., Kim, Y.H., Yu, S.M., Park, S.Y., Yoo, J.B. (2009), "A role of HNO₃ on transparent conducting film with single-walled carbon nanotubes", *Nanotechnology*, **20**, 475703.
- Shyu, F.L. and Lin, M.F. (2000), "Loss spectra of graphite-related systems: A multiwall carbon nanotube, a single-wall carbon nanotube bundle, and graphite layers", *Phys. Rev. B*, **62**, 8508-8516.
- Shockley, W. and Queisser, H.J. (1961), "Detailed balance limit of efficiency of p-n junction solar cells", *J. Appl. Phys.*, **32**, 510.
- Shu, Q., Wei, J., Wang, K., Zhu, H., Li, Z., Jia, Y., Gui, X., Guo, N., Li, X., Ma, C. and Wu, D. (2009), "Hybrid heterojunction and photoelectrochemistry solar cell based on silicon nanowires and double-walled carbon nanotubes", *Nano Lett.*, **9**, 4338-4342.
- Shu, Q., Wei, J., Wang, K., Song, S., Guo, N., Jia, Y., Li, Z., Xu, Y., Cao, A., Zhu, H., Wu, D. (2010),

- “Efficient energy conversion of nanotube/nanowire-based solar cells”, *Chem. Commun.*, **46**, 5533-5535.
- Sivakov, V., Andra, G., Gawlik, A., Berger, A., Plentz, J., Falk, F. and Christiansen, S. H. (2009), “Silicon nanowire-based solar cells on glass: synthesis, optical properties, and cell parameters”, *Nano Lett.*, **9**, 1549-1554.
- Stewart, D.A. and Leonard, F. (2004), “Photocurrent in nanotube junctions”, *Phys. Rev. Lett.*, **93**, 107401
- Sun, J.L., Wei, J., Zhu, J.L., Xu, D., Liu, X., Sun, H., Wu, D.H. and Wu, N.L. (2006), “Photoinduced currents in carbon nanotube/metal heterojunctions”, *Appl. Phys. Lett.*, **88**, 131107.
- Tey, J.N., Ho, X. and Wei, J. (2012), “Effect of doping on single-walled carbon nanotubes network of different metallicity”, *Nanoscale Res. Lett.*, **7**, 548.
- Tombler, T., Zhou, C., Alexeyev, L., Kong, J., Dai, H., Liu, L., Jayanthi, C., Tang, M. and Wu, S. (2000), “Reversible electromechanical characteristics of carbon nanotubes under local-probe manipulation”, *Nature*, **405**, 769-772.
- Tung, R.T. (2000), “Chemical bonding and Fermi level pinning at metal-semiconductor interfaces”, *Phys. Rev. Lett.*, **84**, 6078-6081.
- Tune, D.D., Flavel, B.S., Krupke, R. and Shapter, J. G. (2012), “Carbon nanotube-silicon solar cells”, *Adv. Energy Mater.*, **2**, 1043-1055.
- Tzolov, M.B., Kuo, T.F., Straus, D.A., Yin, A. and Xu, J. (2007), “Carbon nanotube–silicon heterojunction arrays and infrared photocurrent responses”, *J. Phys. Chem. C*, **111**, 5800-5804.
- U.S. Department of Energy (2010), *\$1/W Photovoltaic Systems*, 1-28.
- Venema, L.C., Janssen, J.W., Buitelaar, M.R., Wildöer, J.W.G., Lemay, S.G., Kouwenhoven, L.P. and Dekker, C. (2000), “Spatially resolved scanning tunneling spectroscopy on single-walled carbon nanotubes”, *Phys. Rev. B*, **62**, 5238-5244.
- Wadhwa, P., Liu, B., McCarthy, M.A., Wu, Z., Rinzler, A.G. (2010), “Electronic junction control in a nanotube-semiconducting Schottky junction solar cell”, *Nano Lett.*, **10**, 5001-5005.
- Wang, H., Bai, X., Wei, J., Li, P., Jia, Y., Zhu, H., Wang, K. and Wu, D. (2012), “Preparation of CuI particles and their applications in carbon nanotube-Si heterojunction solar cells”, *Materials Letters*, **79**, 106-108.
- Wang, S., Khafizov, M., Tu, X., Zheng, M., and Krauss, T.D. (2010), “Multiple exciton generation in single-walled carbon nanotubes”, *Nano Lett.*, **10**, 2381-2386.
- Wei, J., Jia, Y., Shu, Q., Gu, Z., Wang, K., Zhuang, D., Zhang, G., Wang, Z., Luo, J., Cao, A. and Wu, D. (2007), “Double-walled carbon nanotube solar cells”, *Nano Lett.*, **7**, 2317-2321.
- Wu, Z., Chen, Z., Du, X., Logan, J.M., Sippel, J., Nikolou, M., Kamaras, K., Reynolds, J.R., Tanner, D.B., Hebard, A.F. and Rinzler, A.G. (2004), “Transparent, conductive carbon nanotube films”, *Science*, **305**, 1273-1276.
- Zeidenbergs, G. and Anderson, R.L. (1967), “Si-GaP heterojunctions”, *Solid State Electron.*, **10**, 113-123.
- Zhang, Z.B., Li, J., Cabezas, A.L. and Zhang, S.L. (2009), “Characterization of acid-treated carbon nanotube thin films by means of Raman spectroscopy and field effect response”, *Chem. Phys. Lett.*, **476**, 258-261.
- Zhou, C., Kong, J., Yenilmez, E. and Dai, H. (2000), “Modulated chemical doping of individual carbon nanotubes”, *Science*, **290**, 1552-1555.
- Zhou, H., Colli, A., Ahnood, A., Yang, Y., Rupesinghe, N., Butler, T., Haneef, I., Hiralal, P. and Nathan, A., Amaratunga, G.A.J. (2009), “Arrays of parallel connected coaxial multiwall-carbon-nanotube-amorphous-silicon solar cells”, *Adv. Mater.*, **21**, 3919-3923.
- Zhou, W., Vavro, J., Nemes, N.M., Fischer, J.E., Borondics, F., Kamaras, K. and Tanner, D.B. (2005), “Charge transfer and Fermi level shift in p-doped single-walled carbon nanotubes”, *Phys. Rev. B*, **71**, 205423.